

Aus der Abteilung für Muskelforschung
am Experimental and Clinical Research Center (ECRC)
Charité – Universitätsmedizin Berlin
Max Delbrück Centrum für Molekulare Medizin (MDC) in der Helmholtz Gesellschaft

DISSERTATION

The effect of chronic constriction injury to the sciatic nerve on myofibrillar
protein synthesis in rat tibialis anterior

zur Erlangung des akademischen Grades
Doctor of Philosophy (PhD)

vorgelegt der Medizinischen Fakultät
Charité – Universitätsmedizin Berlin

von

Henning Tim Langer

aus Berlin

Datum der Promotion: 05.03.2021

Table of content

List of figures and tables	1
Abstract	2
Zusammenfassung	3
1 Introduction	4
1.1 Muscle wasting, quality of life and life expectancy.....	4
1.2 The role of myofibrillar protein turnover in muscle loss.....	4
1.3 Nerve damage as a model to study muscle protein turnover during atrophy.....	5
1.4 Targeted metabolomics, stable isotope labeling and myofibrillar protein turnover	5
2 Methods	7
2.1 Animal studies.....	7
2.2 Immunohistochemistry and -blotting.....	8
2.3 Stable isotope labeling.....	9
2.4 Myofibrillar and plasma protein extraction for GC-MS analysis.....	9
2.5 GC-MS analysis of deuterium enrichment in l-alanine.....	11
2.6 Independent validation of GC-MS results through positive controls.....	11
2.7 Calculations.....	12
2.8 Data analysis and statistics.....	13
3 Results and Discussion	14
3.1 Nerve damage induced type II fiber atrophy.....	14
3.2 Validation of the GC-MS approach through positive controls.....	15
3.3 Myofibrillar protein synthesis is increased during nerve damage and muscle loss.....	16
3.4 Protein synthesis and breakdown signaling.....	19
3.5 Conclusion.....	20
4 Graphical Summary	21
5 References	22
6 Affidavit	26
7 Authors contributions	28
8 Journal summary list	29
9 Publication	30
10 Curriculum vitae	40
11 Complete list of publications	41
12 Acknowledgments	42

LIST OF FIGURES AND TABLES

Figure 1	Localization of GLUT4 and myosin heavy chain-slow in nerve damaged rat tibialis anterior	p14
Figure 2	Deuterium labeled l-alanine enrichment in exercised rat muscle	p15
Figure 3	Fractional myofibrillar protein synthesis rates after nerve damage	p17
Figure 4	Estimated net protein balance after nerve damage	p18
Figure 5	Protein levels of p70S6K1 following nerve damage	p20

ABSTRACT

This doctorate comprised several projects investigating skeletal muscle metabolism in neuromuscular diseases, resulting in multiple publications. Based on the doctoral degree regulations of the Charité Berlin, this dissertation will focus exclusively on the first project that led to a “top journal” publication. In this project I investigated skeletal muscle protein turnover in rat tibialis anterior (TA) following chronic constriction injury to the sciatic nerve. While changes to muscle protein metabolism after nerve transection are relatively well understood, knowledge on other peripheral nerve injuries is sparse. Chronic constriction injury was caused by implanting a cuff tightly around the sciatic nerve of male Sprague-Dawley rats between 21 to 22 weeks of age (n=10). Four weeks after surgically inducing the injury, bodyweight of the animals did not change significantly while body composition was altered. Lean body mass decreased by 3.7 % from 75.4 % (± 2.3 %) to 71.7 % (± 1.3 %) which was accompanied by a concomitant increase in bodyfat by 2.7 % from 18.3 % (± 2.1 %) to 21.2 % (± 2.5 %) ($p < 0.01$, $p < 0.05$). Locally, the constriction injury had caused a decrease in muscle mass of 66 % (± 10 %) and 50 % (± 17 %) of the TA and extensor digitorum longus, respectively ($p < 0.001$, $p < 0.001$). We found that this loss of mass was predominantly caused by a decrease in fiber diameter rather than fiber number: Average fiber diameter of type I fibers in the TA decreased by 38 % ($47 \mu\text{m} \pm 3 \mu\text{m}$ [control] to $34 \mu\text{m} \pm 3 \mu\text{m}$ [damaged]), type II a fibers by 30 % ($47 \mu\text{m} \pm 4 \mu\text{m}$ [control] to $36 \mu\text{m} \pm 7 \mu\text{m}$ [damaged]) and type II b fibers by 70 % ($56 \mu\text{m} \pm 6 \mu\text{m}$ [control] to $33 \mu\text{m} \pm 6 \mu\text{m}$ [damaged]) ($p < 0.01$, $p < 0.05$, $p < 0.001$) while fiber number did not decrease in a statistically significant manner. We used stable isotope labeling via deuterium oxide to investigate changes of myofibrillar protein synthesis during the last two weeks of the intervention. Despite substantial loss of muscle mass and apparent fiber atrophy, myofibrillar protein synthesis was increased in every single animal by an average 55 % in nerve damaged TA compared to the contralateral control leg (3.23 ± 0.72 [damaged] to $2.09 \pm 0.26\% \cdot \text{day}^{-1}$ [control]) ($p < 0.001$). This increase in myofibrillar protein synthesis was supported by a coincstantaneous increase in the protein levels of p70S6K1 by 33 % from 1.8 ± 0.2 to 2.4 ± 0.3 AU ($p < 0.01$). In conclusion, we found that constriction injury of the sciatic nerve is accompanied by a substantial decrease in muscle mass and muscle fiber diameter despite a significant increase in myofibrillar protein synthesis and anabolic signaling protein levels. As such, to ameliorate muscle loss in chronic nerve constriction injury, targeting myofibrillar protein breakdown could hold more promise than targeting the already increased synthesis of myofibrillar proteins.

ZUSAMMENFASSUNG

Diese Promotion befasste sich mit Projekten zum Stoffwechsel der Skelettmuskulatur in neuromuskulären Erkrankungen, wovon mehrere in Publikationen resultierten. Basierend auf der Promotionsordnung der Charité Berlin behandelt diese Dissertation ausschließlich das erste Projekt, aus welchem eine „Top Publikation“ hervorging. Dieses Projekt untersuchte Änderungen des Proteinstoffwechsels in Muskelgruppen, die von chronischer Nervenkonstriktion betroffen sind. Während ähnliche Untersuchungen zu vollständig denervierten Muskeln publiziert sind, ist wenig über den Muskelstoffwechsel in anderen peripheren Nervenverletzungen bekannt. Eine chronische Nervenkonstriktion des N. ischiadicus wurde durch die Implantation einer Manschette um den Nerv 21-22 Wochen alter Sprague-Dawley Ratten (n=10) hervorgerufen. Vier Wochen postoperativ war das Körpergewicht der Tiere unverändert, anders als die Körperkomposition: Die fettfreie Masse reduzierte sich um 3.7 % von 75.4 % (± 2.3 %) auf 71.7 % (± 1.3 %), was von einem gleichzeitigen Anstieg des Fettanteils um 2.7 % von 18.3 % (± 2.1 %) auf 21.2 % (± 2.5 %) begleitet wurde ($p < 0.01$, $p < 0.05$). Lokal verursachte der Nervenschaden eine Reduktion des Muskelgewichtes des M. tibialis anterior (TA) und M. extensor digitorum longus um 66 % (± 10 %) und 50 % (± 17 %) ($p < 0.001$, $p < 0.001$). Diese Reduktion der Muskelmasse ließ sich primär auf Faseratrophie zurückführen: Der Durchmesser der Typ I Fasern reduzierte sich im TA um 38 % ($47 \mu\text{m} \pm 3 \mu\text{m}$ [Kontrolle] zu $34 \mu\text{m} \pm 3 \mu\text{m}$ [Intervention]), der Typ II A Fasern um 30 % ($47 \mu\text{m} \pm 4 \mu\text{m}$ [Kontrolle] zu $36 \mu\text{m} \pm 7 \mu\text{m}$ [Intervention]) und der Typ II B Fasern um 70 % ($56 \mu\text{m} \pm 6 \mu\text{m}$ [Kontrolle] zu $33 \mu\text{m} \pm 6 \mu\text{m}$ [Intervention]) ($p < 0.01$, $p < 0.05$, $p < 0.001$), während sich die Faserzahl nicht signifikant unterschied. Um die Syntheserate von myofibrillärem Protein zu untersuchen, verwendeten wir während der letzten zwei Wochen der Intervention Isotopenmarkierung durch Deuteriumoxid. Trotz des starken Verlustes an Muskelmasse sahen wir einen signifikanten Anstieg der myofibrillären Proteinsynthese von durchschnittlich 55 % im TA des nervengeschädigten Beines (3.23 ± 0.72 [Intervention] zu 2.09 ± 0.26 %*Tag⁻¹ [Kontrolle]) ($p < 0.001$). Jedes Tier zeigte einen Anstieg der Proteinsyntheserate mit der Intervention. Dieser Anstieg der Syntheserate wurde von einer simultanen Zunahme des Signalproteins p70S6K1 um 33 % (1.8 ± 0.2 AU [Kontrolle] zu 2.4 ± 0.3 AU [Intervention] begleitet ($p < 0.01$), welches dafür bekannt ist, die Proteinsynthese und Zellproliferation zu aktivieren. Zusammenfassend demonstriert diese Arbeit, dass chronische Konstriktion des N. ischiadicus zu starkem Muskelschwund und Faseratrophie führt, welche von einem Anstieg der Muskelproteinsynthese und anaboler Signalproteine begleitet wird. Strategien, welche die Proteolyserate von myofibrillärem Protein verlangsamen, könnten daher vielversprechendere Interventionsziele bei Nervenkonstriktion darstellen als jene, die das Verstärken der bereits erhöhten Muskelproteinsyntheserate zum Ziel haben.

INTRODUCTION

1.1 Muscle wasting, quality of life and life expectancy

Skeletal muscle tissue is indispensable for locomotion. Comprising approximately 40 % of the bodyweight, muscle is also the largest organ of the human body and a major determinant of whole body metabolism and resting energy expenditure [1; 2; 3]. Severe loss of muscle mass causes a decrease in strength and functional capacity that may ultimately lead to a decrease in quality of life, independency and life expectancy [4; 5]. Muscle loss can be caused by a number of medical conditions such as heart failure, chronic obstructive pulmonary disease, cancer and neurological diseases [6; 7; 8; 9]. Furthermore, muscle loss is thought to contribute to disease progression in some of these conditions, both directly and indirectly via disuse and decreased activity [10; 11; 12]. The resulting burden for the healthcare system is enormous. It has been estimated that the cost of sarcopenia, the age-associated loss of muscle mass, was \$18.5 billion for the healthcare system of the United States alone in 2000 [13]. These costs are likely to continue to rise, as many countries experience demographic shifts toward older populations. Despite considerable efforts by the scientific community and pharmacological companies, no drug to counteract muscle loss is available yet. So far, resistance exercise and nutritional strategies have emerged as the only safe and effective treatments to ameliorate muscle wasting. However, certain conditions do not permit the use of resistance exercise as an intervention. In comatose patients or after nerve damage, voluntary muscle contraction may be hampered or impossible [14; 15]. Therefore, understanding the mechanisms driving muscle loss is particularly crucial for the development of treatments in such clinical situations where a combination of exercise and nutrition is not applicable.

1.2 The role of myofibrillar protein turnover in muscle loss

To be able to design therapies against muscle loss it is important to have a target. To develop a target, we need to understand the physiological processes driving muscle loss. Conceptually, changes in contractile protein content of skeletal muscle are determined by the net balance (NB) between myofibrillar protein synthesis (PS) and myofibrillar protein breakdown (PB). The accrual of contractile proteins occurs when the rate of PS exceeds the rate of PB, resulting in a positive NB [16]. On the other hand, the loss of contractile protein occurs when PB occurs at a faster rate than PS. Under normal physiological circumstances in adult humans, PS and PB fluctuate depending on physical activity and food intake, resulting in a balanced NB over the course of the day and weeks [17]. With ageing, injuries, inactivity and certain pathologies, NB can become transiently or permanently negative, leading to muscle loss. Such a negative NB can be caused by a decrease in PS, an increase in PB or

both. Being able to distinguish whether a decrease in PS or an increase in PB drives muscle loss is key to understand a pathology and the design of interventions to improve NB. Currently the scientific field appears torn on the question whether changes in protein synthesis or breakdown are the primary cause of muscle loss in most conditions in humans [18].

1.3 Nerve damage as a model to study muscle protein turnover during atrophy

Peripheral nerve injuries are a common clinical problem which can be disease related or trauma induced [19]. Symptoms include, but are not limited to, neuropathic pain, decreased motor function and skeletal muscle atrophy [19]. While consequences of nerve damage are well investigated on the level of transcription and molecular signaling, less is known about the physiology of muscle protein turnover. Moreover, as opposed to the more frequently investigated nerve dissection model, studies on less radical models of nerve damage such as crush injuries or chronic nerve constriction have been primarily focused on neuropathic pain, with very little attention to the repercussions on skeletal muscle [20; 21; 22]. To contribute to the closure of this gap we chose to investigate muscle protein turnover and changes in muscle size in an animal model of chronic nerve constriction injury [22]. Since certain conditions of muscle wasting vary greatly in their underlying biology, it is important to assess each of them individually [23]. This applies particularly to an understudied condition such as chronic nerve constriction. Finding which side of the protein balance is predominantly affected during constriction injury to the nerve will be pertinent to the goal of ameliorating muscle loss in it.

1.4 Targeted metabolomics, stable isotope labeling and myofibrillar protein turnover

Targeted metabolomics via isotope labeling has been a particularly valuable method to study muscle metabolism *in vivo*, first by using radioactive isotopes and later by using stable isotopes [24]. The latter paved the way for a wider application of the technique, as stable isotopes are safe for use in humans and animals. Most elements have multiple isotopes which can be distinguished in stable or unstable and radioactive. These isotopes differ in their number of neutrons resulting in different atomic masses. For example, hydrogen has three naturally occurring isotopes, ^1H (protium), ^2H (deuterium) and ^3H (tritium). Protium accounts for over 99.9 % of the occurring hydrogen on earth, while deuterium accounts for less than 0.02 % and tritium for one atom per 10^{18} atoms of hydrogen (^3H) [25; 26]. The differences in atomic mass between isotopes can be measured by mass spectrometry, allowing to determine the enrichment of the less frequently occurring isotopes in a biological sample. The basic principle of stable isotope labeling is that a metabolite gets ‘tagged’ (i.e. labeled) with the less commonly occurring, stable isotope and becomes the ‘tracer’ [24]. This is done by increasing the enrichment of the less abundant isotope, such as deuterium, in a metabolite of interest. The same

metabolite should be naturally occurring in a sample that is collected, where it is called the ‘tracee’. The tracee is the same metabolite as the tracer, but without an increased enrichment of stable isotopes. If a tracer is added to cell culture *in vitro* or administered to a subject *in vivo*, it is possible to measure the increased enrichments of stable isotopes in a sample via gas chromatography mass spectrometry (GC-MS) [27]. Gas chromatography (GC) separates derivatized metabolites by volatility. After the GC part, these metabolites are ionized and fragmented during the mass spectrometry (MS) part. Each of these fragments has a mass that is measured by MS and quantified as “mass to charge ratio – m/z” [28]. Depending on the derivatization process, each metabolite has one or multiple characteristic masses and by quantifying the peaks from characteristic masses in a sample, it is possible to calculate its concentration. For example, l-alanine has the characteristic masses 158, 232 and 260 m/z respectively, if derivatized with N-tert-Butyldimethylsilyl-N-methyltrifluoroacetamide (MTBSTFA) [29]. As mentioned above, however, each metabolite has a certain natural abundance of stable isotope elements. These appear with a shift in mass towards a slightly heavier m/z than the characteristic mass and are referred to as “m+1”, m+2”, “m+3” et cetera. To assess the enrichment of a stable isotope such as deuterium in l-alanine with its characteristic mass of 232 m/z, the abundance of the masses 233 (m+1), 234 (m+2) and 235 (m+3) would have to be quantified. These shifts in mass reflect that either one, two or three protium atoms (^1H) have been replaced with deuterium (^2H) [30]. By taking several samples from different tissues at different time points, we can follow the fate of the tracer and calculate incorporation rates [31]. In case of protein synthesis rates and deuterium, the stable isotope (deuterium) can be administered orally or intravenously via deuterium oxide (D_2O), causing a rapid rise of deuterium in the circulation and the labeling of circulating amino acids such as the aforementioned l-alanine. Over time, l-alanine will be incorporated into the protein of tissues such as the liver, kidneys or skeletal muscle [32]. By measuring the change in enrichment of deuterium labeled l-alanine between the circulation and muscle over time (‘precursor pool method’), fractional synthetic rates of the labeled amino acid into muscle can be calculated [33; 34]. Given the assumption that incorporation of new amino acids into muscle protein reflects the *de novo* synthesis of muscle protein, this yields muscle protein synthesis rates [31]. I utilized stable isotope labeling via D_2O to label l-alanine and measure enrichments in the myofibrillar protein fraction of rat TA. I combined this approach with direct assessments of changes in muscle mass as well as histological analysis of fiber diameter and number. This allowed me to obtain data on the relationship between myofibrillar protein synthesis and changes in muscle mass after constriction injury to the sciatic nerve, yielding new insights into the dynamics of muscle protein turnover in this condition.

METHODS

2.1 Animal studies

All animal experiments were approved by the local authority of the Landesamt für Gesundheit und Soziales (LAGeSo) Berlin, under the reference G 0083/15. Nerve damage and muscle atrophy were caused by chronic constriction injury to the sciatic nerve of male Sprague-Dawley rats [22]. The damage to the nerve was unilateral, allowing for the contralateral muscles to serve as healthy, internal control. Rats at an adult age of 21-22 weeks (n=10) were individually housed and fed a balanced diet equivalent to $79 \text{ kcal} \cdot \text{day}^{-1}$ (ssniff Spezialdiäten GmbH, Soest, Germany) (see publication [35] for details). The amount of energy required by the animals for weight maintenance was previously determined in pilot experiments and suited towards avoidance of weight gain commonly associated with *ad libitum* food intake in laboratory animals. Damage to the sciatic nerve was induced by surgically implanting a tight electrode cuff above its point of trifurcation, causing chronic constriction injury to the nerve and muscle atrophy to the muscle groups distal of the injury as described previously [22]. Nerve damage induced muscle loss has been reported to follow a slope that is characterized by rapid, nonlinear muscle loss within the first two weeks and a more linear, continuous muscle loss in the subsequent weeks for up to twelve months following injury [36; 37; 38]. Animals were collected four weeks after initiation of the injury to the nerve (28 days post-surgery). To accommodate our methodological approach and the calculations outlined below (see 2.3 and 2.7), stable isotope labeling and the investigation of muscle protein turnover was conducted during the second half of the intervention (14-28 days post-surgery), when muscle loss followed a more linear pattern. Body composition was measured with a Minispec LF90 II time domain NMR analyzer (6.5 mHz, Bruker Optics, United States). For a more detailed description of the nerve damage model, please see the publication attached to this dissertation and references [22; 35].

As part of an experiment to validate our technological approach to measure muscle protein synthesis via GC-MS (further described under 2.5), we conducted a pilot study in which we exercised a small number of rats (n=4) according to a resistance exercise-like protocol known to activate muscle anabolism and protein synthesis [39; 40]. For this purpose, age-, weight-, and sex matched littermates of the rats designated for the chronic constriction injury protocol were used. Similar to the nerve constriction intervention, the rats of the exercise intervention underwent surgery and an electrode cuff was implanted onto the sciatic nerve above the point of trifurcation. Instead of wrapping the cuff tightly around the nerve to cause a constriction injury, however, the cuff for these animals was gently placed around the nerve with only the platinum wires making light contact with the nerve instead of

constricting it. After surgery, the animals were left to recover for two weeks before the exercise protocol was initiated. The lower limb of each animal was unilaterally exercised for two weeks as described previously [40]. Briefly, the nerve was electro-stimulated at 4-8 V causing a lengthening contraction of the TA and extensor digitorum longus on the stimulated side, while the contralateral leg served as an internal control. This process was repeated for a total of 60 contractions with a minute rest after every sixth contraction (i.e. ten sets of six contractions). Four weeks after the surgery, the animals were collected for tissue analysis (28 days post-surgery). Stable isotope labeling was conducted during the exercise period (14-28 days post-surgery). As such, the exercised animals were labeled for the same duration as the chronic constriction injury animals. However, instead of being exposed to a stimulus causing muscle loss they were exposed to a stimulus known to increase muscle protein synthesis and growth, providing a positive control for our nerve damage experiments.

A set of age-, sex- and weight matched littermate rats (n=3), which did not undergo any intervention, were used to provide unlabeled background values for the GC-MS analysis (see 2.4).

2.2 Immunohistochemistry and -blotting

Immunohistochemistry was performed as described previously with slight modifications [41]. Briefly, freshly cut sections of TA were left 1 h at room temperature to dry and then fixated in 3.7 % paraformaldehyde. After washing, sections were blocked in PBS (3 % BSA). Subsequently sections were incubated with the primary antibodies for 1 h at room temperature and the secondary antibodies were applied overnight, before the process was repeated on the next day in order to stain for both, GLUT4 and Myosin Heavy Chain-slow (MHCs) simultaneously. Nuclei were stained for with Hoechst (Sigma-Aldrich, Germany) before being mounted on slides using Aqua Mount (Thermo Fisher Scientific, Germany). For a more detailed description of the immunohistochemistry protocol and a list of the concentrations and suppliers of the antibodies, please see the publication attached [35].

Western blotting was carried out with approximately 400 μm of muscle sections acquired during the trimming of samples for immunohistochemistry. Protein concentrations were measured and samples were normalized using a standard bicinchoninic acid assay kit (Thermo Fisher Scientific, Germany). Proteins were separated through electrophoresis on sodium dodecyl sulfate gels (Thermo Fisher Scientific, Germany) that ran at 200 V for 45 min, before the proteins were transferred for 45 min at 18 V using the semi dry blot technique. Primary antibodies were applied with varying concentrations in tris-buffered saline with tween and milk or bovine serum albumin overnight at 4° C. Secondary antibodies were applied for 60 min at room temperature on the following day. For quantification, all

protein levels were normalized to total protein content per lane as assessed via Ponceau S staining since this was shown to be more reliable than the use of housekeeping proteins [42]. For a more detailed description of western blotting, please see the publication attached [35].

2.3 Stable isotope labeling

Animals were stable isotope labeled via deuterium oxide using previously published protocols with modifications [32; 43]. Endogenous deuterium water levels were raised to 4 % by intraperitoneal injection of 0.014 mL *g⁻¹ bodyweight deuterium oxide (99.8 % + Atom D, Euriso-Top GmbH Saarbrücken) and 0.9 % NaCl. Body levels were maintained via drinking water (4 % deuterium oxide). The stable isotope labeling was started two weeks after surgery and maintained for two weeks until the animals were collected (i.e. 14 to 28 days post-surgery). A set of unlabeled rats served as a control (see 2.1). Stable isotope enrichment in the myofibrillar protein fraction was investigated via GC-MS (see 2.4 to 2.8 for details). This method of measuring enrichments of deuterium in amino acids such as l-alanine has a rich history in the literature and has been validated in cell culture and *in vivo* extensively [30; 44; 45; 46]. It has been successfully applied to measure protein turnover rates in several types of tissues in rodents and humans via GC-MS, in acute settings as well as over the course of multiple weeks [43; 47; 48].

2.4 Myofibrillar and plasma protein extraction for GC-MS analysis

To measure the l-alanine enrichment in the myofibrillar protein fraction of nerve damaged rat TA, ice-cold buffer was added to each sample before they were homogenized and the myofibrillar protein fraction extracted as described previously [49; 50]. To separate the sarcoplasmic fraction from the fraction rich in myofibrillar proteins, each sample was spun at 700 g for 10 min at 4° C. The remaining pellet was washed twice, once with the buffer and once with dH₂O. Afterwards 1 mL of 0.3M NaOH was added to the pellet to further improve solubilization of the myofibrillar proteins and to separate them from collagen in the sample. The samples were then heated for 30 min at 50° C and subsequently spun at 10,000 g for 5 min at 4° C before the supernatant containing the myofibrillar proteins was transferred into 4 mL screw-cap glass vials. To denature the myofibrillar proteins, 1mL of 1M PCA was added to each glass vial. Following another centrifugation step, the supernatant was removed and the pellet washed twice with 500 µL 70 % EtOH. After discarding the EtOH and drying the pellet, 1.5 mL of 6M HCL was added to the pellet to hydrolyze it and liberate the amino acids overnight in an oven at 110° C. On the following day, the samples were transferred to a heating block (120° C) and dried under a nitrogen steam. To further purify the samples and isolate the amino acids, the samples were passed through a Dowex exchange resin (AG 50W-X8 Resin, Bio-Rad, USA) before the

derivatization step. After purification, the vials with the samples were carefully vortexed and dried under a nitrogen stream before derivatization. For derivatization, 50 μ L of N-tert-Butyldimethylsilyl-N-methyltrifluoroacetamide (MTBSTFA) (Sigma-Aldrich, Germany) and 50 μ L of acetonitrile were added to each sample to convert them to their tert-butyldimethylsilyl (TBDMS) derivatives. MTBSTFA has been shown to be the most reliable derivatization reagent for the analysis of amino acids via GC-MS as derivatives are more stable and less moisture sensitive than those formed with reagents such as N,O-Bis(trimethylsilyl)trifluoroacetamide (BSTFA) [51]. Each sample was incubated for 1 h at 70° C. Samples were then transferred to 2 mL screw-cap chromacol vials (Thermo Fisher Scientific, Schwerte, Germany) for GC-MS injection.

To calculate incorporation rates of deuterium into myofibrillar proteins, changes in enrichment in the precursor pool need to be measured alongside the myofibrillar concentrations. Plasma protein is commonly used as a precursor pool for this purpose [52; 53]. Plasma protein of rats was precipitated by adding 40 μ L perchloric acid (20 %) to 360 μ L of plasma. We separated free amino acids from protein bound amino acids by centrifugation (3500 rpm, 20 min, 4°C). Pellets were collected and washed three times in 1 mL perchloric acid (2 %) before being hydrolyzed over night as described above. Samples were purified and processed for GC-MS injection as described above. Unlabeled control samples (plasma and muscle) of age-, sex and weight matched rats were run alongside labeled samples on the GC-MS for baseline values and background subtraction of isotope enrichment (see 2.1 and 2.3).

2.5 GC-MS analysis of deuterium enrichment in l-alanine

The analysis of deuterium enrichment in l-alanine via GC-MS was carried out at the Stable Isotope Research Center (SIRC) (Maastricht University, Netherlands). A 6890N GC coupled with an inert 5973N mass selective detector (MSD) (Agilent, USA) was used for electron ionization gas chromatography-mass spectrometry. To assess enrichment of deuterium in alanine, selected ion monitoring (SIM) of the masses 232, 233, 234, 235 and 236 m/z was performed as described previously [54; 55]. Samples were injected in split mode (75:1) using a temperature-controlled injector (Gerstel, Germany) with a glass inlet liner (Agilent, Australia). Gas chromatographic separation was performed on an Agilent 6890 N (Agilent, USA) equipped with a DB-5MS column (30 m x 0.25 mm, d_f 0.25 μ m; J&W, USA). Helium was used as carrier gas at a constant rate of 1 ml/min flow. Gas chromatography was performed starting at an initial temperature of 80 °C for two minutes, gradually increasing up to 300 °C. Detector voltage was set to 1224 V. Standard regression curves for l-alanine concentration and isotopic enrichment of deuterium in l-alanine were applied to assess linearity of the mass spectrometer

and to control for the loss of tracer. Data was acquired and processed using the vendor software Agilent MSD ChemStation version D.03.00 (Agilent, USA). Mole percent excess were calculated by normalizing the enrichment values of stable isotope labeled samples to unlabeled background samples of plasma or muscle, using the calculations outlined in 2.7. Background samples of unlabeled age, weight and sex matched littermate rats were prepared alongside labeled samples as described in 2.4.

2.6 Independent validation of GC-MS results through positive controls

In order to confirm our methodological approach and exclude the possibility of batch effects, we measured a set of positive control samples (see 2.1, second paragraph) on two separate GC-MS: The Agilent 6890N GC/5973N MSD at the SIRC (Maastricht, Netherlands) (see 2.5) and an Agilent 6890N coupled to a time of flight - mass spectrometer (Pegasus III – TOF-MS System (LECO, USA)) at the Berlin Institute of Medical Systems Biology (BIMSB) (Max Delbrück Center Berlin, Germany). To validate our ability and sensitivity to measure changes in muscle protein synthesis, we used TA tissue of rats that were exercised unilaterally according to a protocol known to increase protein synthesis [39; 40]. We prepared all samples (i.e. of the nerve damage- and the exercise intervention) simultaneously as described under 2.4 up to the point of derivatization. Derivatization was then carried out at the two different sites of the machines. The run on the GC-MS in 2.5 was executed as described in the same section. The run on the GC-TOF-MS was conducted with identical settings unless stated otherwise: Helium was used as carrier gas at slightly faster, constant flow rate of 1.2 ml/min. Gas chromatography was performed starting with a slightly lower temperature of 68 °C for two minutes, gradually increasing up to 320 °C. Detector voltage was set to 1520 V. The data were processed with the vendor software ChromaTOF (LECO, USA) including resampling, baseline subtraction and peak detection. Enrichments were normalized to known standards as described in 2.6 and mole percent excess were calculated as detailed in 2.7.

2.7 Calculations

To quantify the deuterium l-alanine enrichment in each sample, the tracer to tracee ratios (TTR) and mole percent excess (MPE) were calculated according to the following formulas [56]:

$$\text{TTR} = \text{Sample TTR} - \text{Background TTR}$$

where the “tracer to tracee ratio” (TTR) is the quotient of the peak intensity of the mass 233 m/z of l-alanine (“tracer”, m+1) and the peak intensity of mass 232 m/z (“tracee”, m+0). Sample TTR is the quotient of the aforementioned intensities in a muscle sample from an animal that underwent the stable

isotope labeling protocol detailed in 2.3, while background TTR is the same quotient in a sample from age and sex matched animals that were not labeled. Subtracting the background from a labelled sample allows to correct for the natural occurrence of stable isotopes in a sample. Based on limitations of accurately detecting lower isotope enrichments with conventional GC-MS (as opposed to isotope ratio mass spectrometry (IRMS)), the m+1 (233 m/z) to m+0 (232 m/z) ratio is commonly used to calculate TTR rather than the ratio of heavier isotopomers (i.e. m+, m+3 and so forth) to m+0 [52]. To transform TTR to MPE, which is more accurately describing isotopic enrichment, the following formula was used [56]:

$$MPE = TTR / (1 + TTR) \times 100$$

where TTR is the value obtained in the calculation above and MPE is expressed in percent. Based on the precursor-product equation, the fractional synthesis rate of a protein can be computed by calculating the change of enrichment in protein bound tracer divided by the change of enrichment in the precursor pool, multiplied by the time of the intervention and 100 to convert into percent [57]:

$$FSR (\% * day^{-1}) = \frac{EM2 - EM1}{(EP - EP1) * t} * 100$$

where FSR is fractional synthetic rates in percent per day, EM2 is the enrichment in myofibrillar protein bound deuterium at the end of the intervention, EM1 is the enrichment in myofibrillar protein bound deuterium before the start of the intervention (i.e. muscle background sample), EP2 is the enrichment of protein bound deuterium in the precursor protein pool (i.e. plasma protein) at the end of the intervention, EP1 is the enrichment of plasma protein bound deuterium before the start of the intervention and t is the duration of the intervention in days. To gain further insight into the dynamics of muscle protein turnover during nerve damage, we applied a previously published calculation with modifications to obtain an estimate of myofibrillar protein breakdown [58]:

$$NB = PS - PB$$

where NB is the myofibrillar net protein balance, PS is the myofibrillar fractional synthetic rate and PB is the myofibrillar fractional breakdown rate. This calculation relies on the measurement of PS and changes in muscle size (as a proxy for NB) to deduce an estimate for PB [58; 59].

Data analysis and statistics

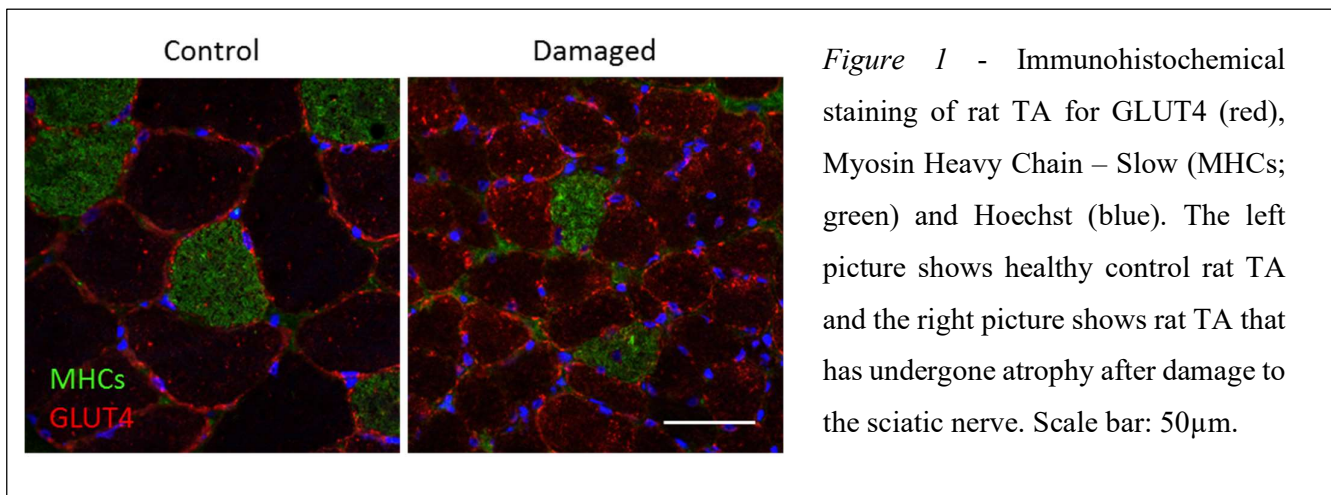
Data of the 6890N GC-5973N MSD at the SIRC (Maastricht University, Netherlands) was acquired in SIM mode and processed using the vendor software Agilent MSD ChemStation (Agilent, USA). Peaks were identified and integrated using ChemStation including baseline correction, identification of retention indices and analysis of peak height. Mass spectra were identified by using the probability-based matching algorithm (PBM) of the ChemStation software and the NIST library [29]. Quantification was performed in two steps, first by setting up a calibration curve and creating a quantitation database through deuterium and l-alanine standards that were run alongside samples (see 2.5). Calibration curves were generated as linear regression fit of the data points. The second step was to normalize the peak heights in samples to those of the standards using the quantitation database. Metabolite identification and peak analysis of the GC-TOF-MS data at the BIMSB (Max Delbrück Center, Germany) was performed using the ChromaTOF vendor software (LECO, USA). Pre-processing of the data consisted of resampling (sample reduction rate of 4 and Mass bins of 70-600), baseline subtraction (baseline offset of 1, peak width of 4s) and peak detection (signal to noise of 50 and 12 data points for peak smoothing). Retention indices were calculated based on retention index standards (nine different alkanes) that were run alongside the samples as described previously [60]. The NIST database provided mass spectra and retention information for peak identification [29]. Quantification was carried out by using the quantification routine of ChromaTOF for external calibration based on measured standards. Standard regression curves of standards for concentration of l-alanine and isotopic enrichment of deuterium in l-alanine were calculated to ensure linearity of the data and account for the loss of tracer, similar to the workflow at the SIRC described above. Using the “peak true intensity” tool in ChromaTOF, the intensity of the peaks for 232, 233, 234 and 235 m/z was determined manually in the l-alanine mass spectrum of every sample. Statistical analyses of all data were performed using Microsoft Excel and GraphPad Prism (San Diego, USA). Data are expressed as mean \pm standard deviation. Student’s t test or one way ANOVA with Tukey’s post hoc test were applied depending on the number of groups to test the null hypothesis. P-values below 0.05 were deemed significant.

RESULTS AND DISCUSSION

3.1 Nerve damage induced type II fiber atrophy

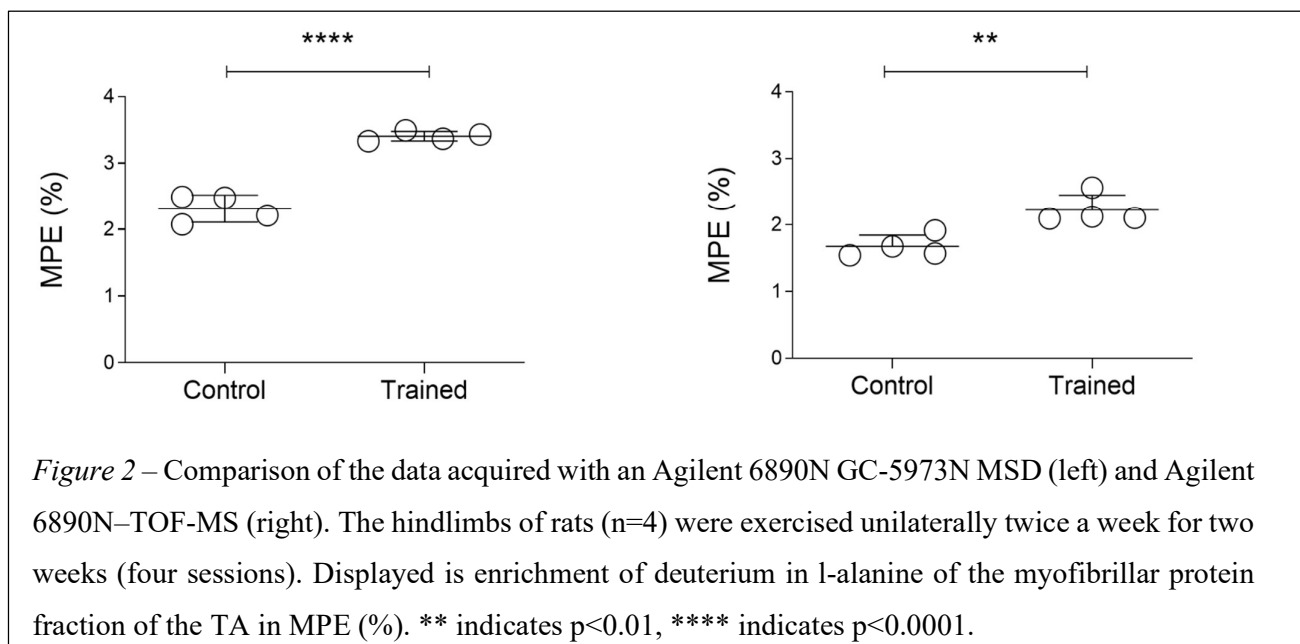
Chronic constriction injury to the sciatic nerve led to a 66 % (± 10 %) loss of muscle mass in TA muscle of otherwise healthy SD rats 28 days following surgery [35]. Histological analysis revealed signs of myopathy with regenerating fibers, centrally located nuclei, necrotic and atrophic fibers (Figure 1) [35]. Mean Feret's diameter in healthy type I fibers of the TA was 47 μm (± 3 μm) compared to 34 μm (± 3 μm) in damaged fibers [65]. Clustered analysis of type II a and -b fibers showed a decrease from 52 μm (± 7 μm) to 35 μm (± 6 μm) in healthy and nerve damaged TA, respectively. Even though a decrease in fiber diameter was apparent in both fiber types, the loss was statistically more pronounced in type II fibers [65]. This is in line with other publications on muscle atrophies of different origins, showing that the loss of muscle mass is often predominantly due to type II fiber atrophy [23; 61]. I counted the total number of fibers in a complete cross section of control and nerve damaged TA. I found no significant difference in fiber number between damaged and healthy TA [35]. These data indicate that the decrease in muscle mass was due to loss of individual fiber size rather than reduction of fiber number, consistent with muscular atrophy as opposed to dystrophy.

In respect to systemic changes of body composition, lean body mass had decreased by 3.7 % from 75.4 % (± 2.3 %) to 71.7 % (± 1.3 %) four weeks after surgery, which was accompanied by a simultaneous increase in bodyfat by 2.7 % from 18.3 % (± 2.1 %) to 21.2 % (± 2.5 %) ($p < 0.01$, $p < 0.05$). Meanwhile, bodyweight of the rats did not change significantly from the start until the end of the intervention, indicating that the changes in body composition are unlikely to be age related.



3.2 Validation of the GC-MS approach through positive controls

To test our methodological approach of analyzing stable isotope enrichment in muscle tissue via GC-MS, we conducted a control experiment independent from the nerve constriction injury intervention. To validate our ability to measure changes in tracer enrichments and in myofibrillar protein synthesis, we exposed rats to an exercise stimulus known to increase muscle protein synthesis, anabolic signaling and muscle size [39; 40]. Rats were trained unilaterally twice a week for two weeks, while the contralateral leg served as a control. Since this protocol is known to increase muscle protein synthesis, our GC-MS measurements should show an increase in MPE in the trained leg compared to the control leg. Indeed, the results obtained with the GC-MS as detailed under 2.5 showed a robust increase of 47 % in the trained TA (3.4 ± 0.07 MPE) compared to the control side (2.32 ± 0.21 MPE) ($p < 0.0001$) (Figure 2). To test the reproducibility of our results, we performed a separate analysis of the same set of samples on a different GC-MS (Pegasus III – TOF-MS System) (see 2.6). Despite slight differences in specifications and the types of mass spectrometers, the results obtained were similar. We found an increase of 32 % in the trained TA (2.22 ± 0.23 MPE) compared to the control leg (1.68 ± 0.17 MPE) ($p < 0.01$) (Figure 2). Overall, the enrichments of deuterium in l-alanine of the myofibrillar fraction obtained by the GC-TOF-MS system were slightly lower than the Agilent 6890N GC/5973N MSD. However, with both machines we were able to detect a robust increase in enrichment in every single sample (Figure 2). For any further data analysis we chose to use the results from our measurements at the SIRC, as they were slightly closer to those reported in the literature [43]. The data presented in the following paragraphs (Figure 3 and 4) was obtained with the Agilent 6890N GC/5973N MSD at the SIRC.

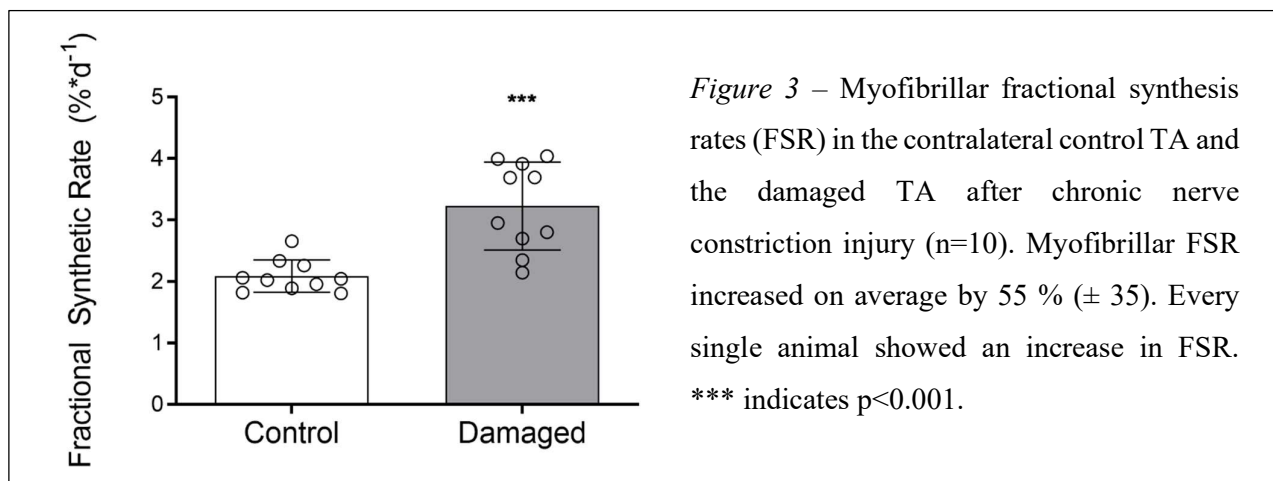


3.3 Myofibrillar protein synthesis is increased during nerve damage and muscle loss

To investigate whether changes to muscle protein synthesis, breakdown or both drive the observed decrease in muscle mass and fiber size with chronic constriction injury to the nerve (Figure 1 and [35]), we used stable isotope labeling of skeletal muscle tissue. Four weeks after constriction injury to the sciatic nerve, rat TA was collected and processed according to the methods detailed in 2.3, 2.4 and 3.2. Stable isotope labeling via deuterium oxide was only applied for week three and four (i.e. the last two weeks of the intervention). This time frame was chosen for two reasons. First, nerve damage associated muscle atrophy tends to follow an exponential pattern for the first days up to two weeks, after which the rate of muscle loss becomes more linear [36; 38]. Since we were interested in the chronic changes occurring with constriction injury to the nerve, measuring myofibrillar protein synthesis over the first weeks would likely only poorly reflect changes to muscle mass. A similar effect has been reported for the opposite scenario (exercise and muscle growth): acute myofibrillar protein synthesis after one week of resistance training does not correlate with chronic changes in muscle size. However, after the initial injury response and a steep increase in synthesis during the first week, myofibrillar protein synthesis during the third and tenth week of training starts to correlate closely with changes in muscle mass [62]. Therefore, to avoid any surgery induced acute injury responses and steep increases of protein synthesis during the first two weeks of our intervention, we chose to analyze myofibrillar protein synthesis during week three and four after constriction injury to the nerve. The second advantage of using a situation closer to steady state is related to the tracer calculations detailed under 2.7. In a non-steady state situation, fractional synthetic rate is commonly calculated by using a non-linear least squares curve fitting formula assuming rise to plateau kinetics [31; 52]. Such a situation arises if the protein of interest is known to have a particularly high turnover rate or the intervention is particularly long [43]. Neither is the case in our intervention, where we avoided the early, rapid changes to muscle size which are likely associated with extreme changes to protein turnover and instead chose a time where muscle loss follows a more linear pattern according to the literature [36] and our own pilot experiments (data not shown). In addition, muscle is known to have a relatively slow turnover rate compared to other tissues [63]. As such, in the scenario of our study the standard precursor product calculation should yield a valid estimation of myofibrillar protein synthesis rates and at the same time allow us to monitor changes to myofibrillar protein synthesis after constriction injury in a manner that reflects chronic, rather than acute changes to muscle mass [52].

During this designated time frame after initiating chronic constriction injury to the nerve (i.e. week three and four post-surgery), myofibrillar fractional synthetic rates (FSR) in the TA were increased 1.6 fold in the damaged compared to the control leg (3.23 ± 0.72 to 2.09 ± 0.26 %*day⁻¹, respectively)

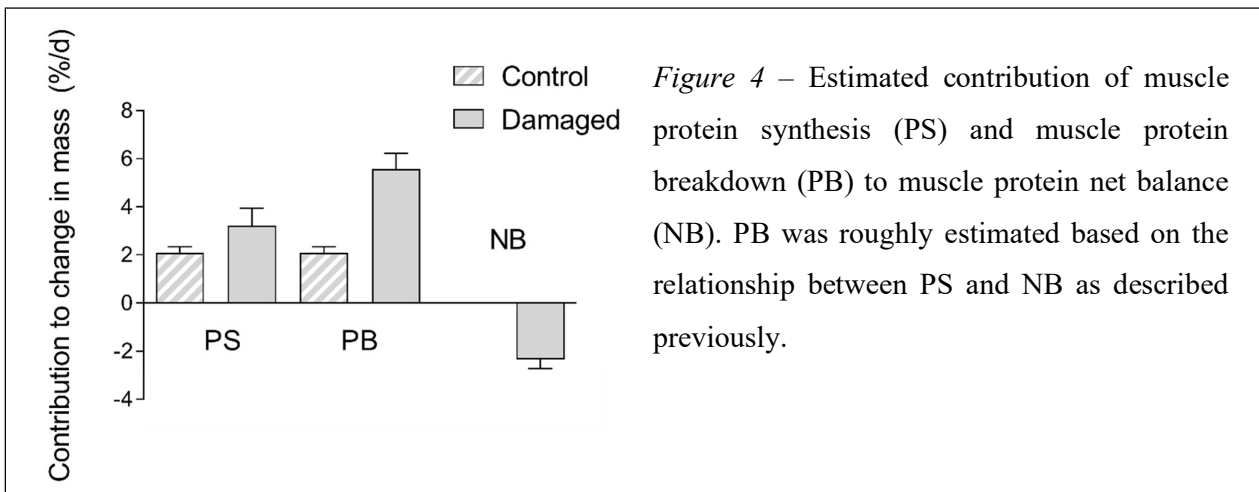
(Figure 3) [35]. While the amplitude of the increase in myofibrillar FSR was variable, every single animal (n=10) showed increased FSR values in the damaged compared to the control leg [35]. We found a concomitant decrease in muscle mass of 66 % (± 10 %) in the nerve damaged TA compared to the control leg over the course of the entire intervention, indicating that a decrease in the synthesis of contractile muscle proteins is unlikely to drive atrophy after chronic nerve constriction. This is in contrast to research that has suggested decreased muscle protein synthesis as the primary mechanism in muscle wasting [16; 64]. Most of the data underlying this view, however, were collected in immobilized or elderly subjects undergoing healthy ageing [12; 65; 66; 67]. In line with our findings, early research in rats after nerve transection had shown increased muscle protein synthesis rates despite “relative atrophy” [38; 68]. Yet, as distinct from our experiments, these animals were particularly young and underwent age related growth. This caused an increase in the absolute muscle mass of the denervated muscles over the course of the experiment. Therefore, the phenomenon investigated in those studies appears to be slowed growth rather than “relative atrophy”. Considering the situation of systemic as well as local growth in those studies, increased muscle protein synthesis rates might be less surprising. In case of our experiments, the rats were fully grown (21-22 weeks old) and underwent absolute atrophy of the TA affected by nerve constriction compared to the contralateral control leg (350 ± 96 to 1037 ± 147 mg, respectively). To the best of our knowledge, this is the first study showing increased myofibrillar FSR during a prolonged period of absolute muscle loss. Confirming other recent findings, this suggests that myofibrillar FSR alone is an indicator of muscle remodeling and regeneration rather than changes to muscle size [62; 69].



While myofibrillar protein synthesis (PS) can be reliably measured using stable isotope tracers, myofibrillar protein breakdown (PB) is more elusive. Even though methodological solutions have been described, they are technically challenging and reliable data on muscle protein breakdown remains sparse [70]. However, to understand what drives changes in muscle mass PB is indispensable. To gain

conceptual insight into the nature of muscle protein turnover during nerve damage, we employed a previously published approach to calculate a rough estimate of PB [58]. This approach has been used to assess PB in animal models and more recently in humans [58; 59]. The calculation integrates changes in PS and muscle mass to derive an estimated value for PB. In this model, change in muscle mass is assumed to directly reflect myofibrillar net protein balance (NB). Since NB is the result of PS minus PB, knowing values for NB and PS allows to deduce a value for PB [58]. To obtain such an estimation for PB, we applied this simple method and divided the total loss of TA mass (i.e. 66%) by the number of days between surgery and sacrifice of the animal (i.e. 28 days), yielding the average loss of TA mass per day (2.35 ± 0.35 %*day⁻¹) (NB) (Figure 4). Integrating this proxy for NB with the PS data (Damaged TA: 3.23 ± 0.72 ; Control TA: 2.09 ± 0.26 %*day⁻¹), PB is estimated to be increased approximately 2.7-fold in the nerve damaged TA compared to the control TA (Damaged: 5.58 ± 0.65 ; Control: 2.09 ± 0.26 %*day⁻¹) (Figure 4).

A caveat of this calculation is the aforementioned course of muscle loss following nerve damage: while eventually following a linear pattern, tissue is initially lost at a more rapid rate [36; 38]. Therefore, our value for average muscle loss per day likely underestimates the rate of early muscle loss and overestimates the rate of muscle loss at later stages. Since we measured myofibrillar protein synthesis during the last two weeks of the intervention (week three and four post-surgery) and net protein balance is likely less negative at this point, the calculation is likely to slightly overestimate the contribution of myofibrillar protein breakdown (PB) to chronic muscle loss our model of nerve damage. However, despite these limitations it still allows for a conceptual illustration of the dynamics of muscle protein turnover during chronic constriction injury to the nerve: since myofibrillar protein synthesis is increased despite continuous loss of muscle mass, substantially increased muscle protein breakdown appears to be the main driver of a negative NB in this model of muscle loss.



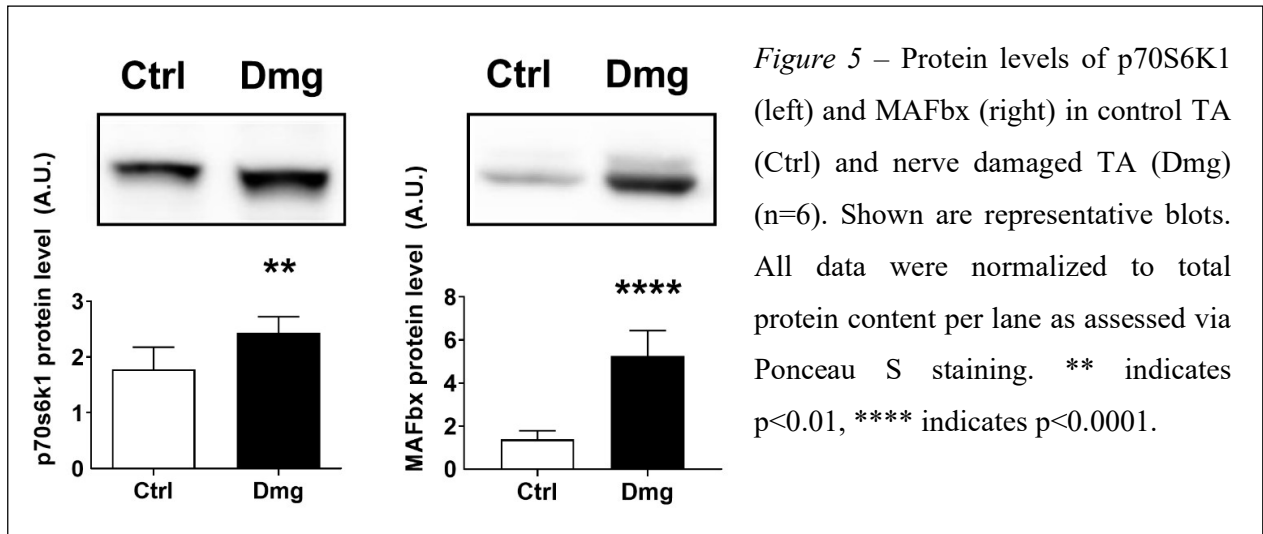
3.4 Protein synthesis and breakdown signaling

To investigate the molecular pathways underlying the changes we found in muscle protein turnover, we performed immunoblotting of some of the main signaling proteins involved in muscle protein synthesis and breakdown. For muscle protein synthesis we focused on p70S6K1, a protein downstream of mTORC1, which is known to increase protein synthesis upon phosphorylation and has a regulatory role in muscle growth [40; 71]. To gain insight into the signaling underlying increased muscle protein breakdown, we analyzed the E3 ubiquitine ligases MAFbx/Atrogin-1 and MuRF1. These are muscle specific proteins downstream of FOXO, which have been shown to be upregulated under most atrophic conditions and are crucial regulators of proteolysis and muscle loss [72].

In our model, protein levels of p70S6K1 increased by 40 % from 1.8 ± 0.2 to 2.4 ± 0.3 AU in the nerve damaged leg compared to the control leg (Figure 5) ($p < 0.01$). Since for the activation of p70S6K1 phosphorylation is required, we tried to analyze phospho-p70S6K1, but failed to detect any in both the damaged and the control legs. However, the lack of phosphorylated p70S6K1 is not surprising, as the protein level pattern is transient and sampling of muscle has to occur closely to the initiation of the stimulus, which was not the case in our study [39; 73]. Supporting a crucial role for timing, we did find increased levels of phosphorylated p70S6K1 when we analyzed the samples of our pilot experiment of exercised rats (described under 2.1), where the collection of the tissue occurred within 48 hours of the last exercise stimulus (data not shown). However, not only phosphorylated but also total levels of p70S6K1 are increased in scenarios of increased protein synthesis and muscle growth. For example, during compensatory muscle hypertrophy following synergist ablation, total protein levels of p70S6K1 are increased [74]. Similarly, during transient hypertrophy of the hemidiaphragm following acute denervation, total levels of p70S6K1 were reported to be increased [75]. Therefore, while phosphorylation of p70S6K1 is more indicative of initiation of protein synthesis, increased levels of total p70S6K1 are more likely to reflect an increased potential of muscle protein synthesis and chronic changes in muscle size depending on the activity of proteolytic processes.

In respect to signaling proteins governing proteolysis, levels of both MAFbx and MuRF1 were increased in the nerve damaged leg compared to the control leg [35]. An important limitation regarding MuRF1, however, is the reliability of the antibody. The MuRF1 antibody was reported to produce unspecific bands casting doubt on the specificity of this antibody, leading us to report only the MAFbx results (Figure 5) [35; 76]. MAFbx levels were increased markedly from 1.4 ± 0.4 to 5.3 ± 1.2 AU in the nerve damaged TA compared to the control leg (Figure 5). This equals a 380 % increase in a signaling protein crucially involved in muscle protein breakdown, compared to the 40 % increase we

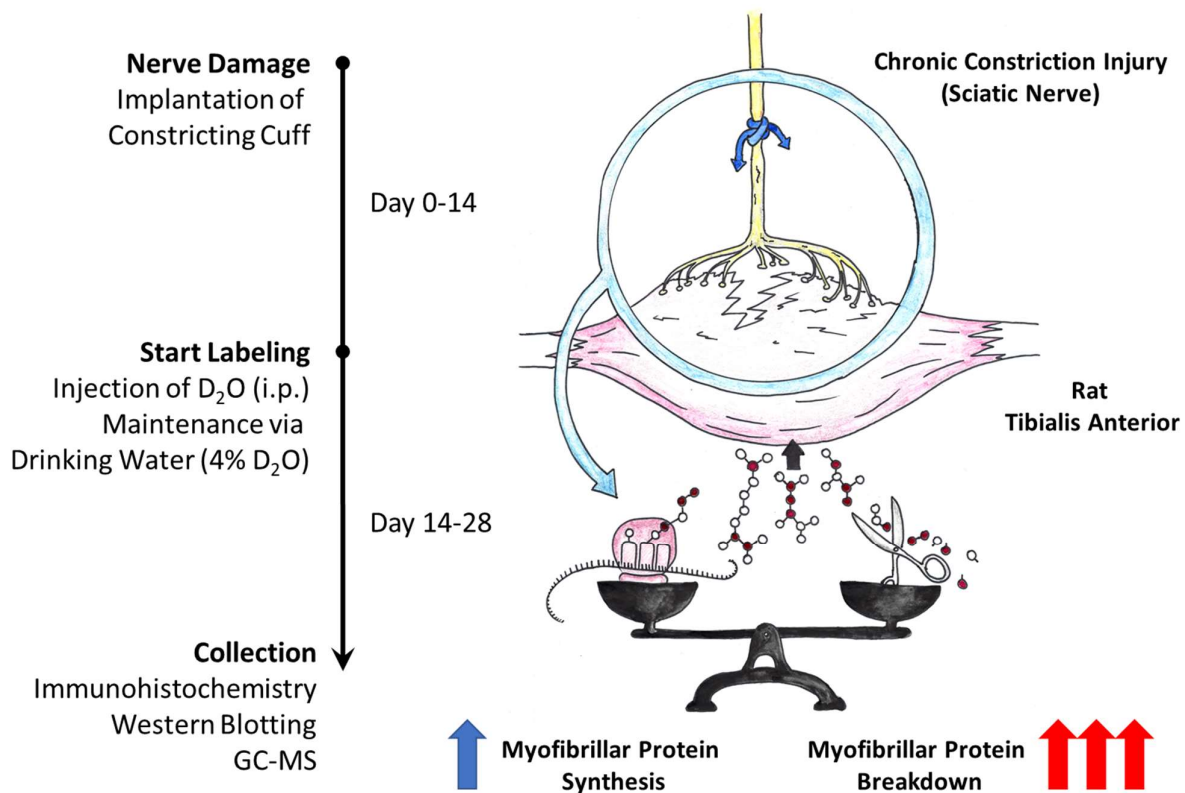
found in total p70S6K1, a protein involved in the signaling of muscle protein synthesis. This supports the stable isotope data where we found a very consistent, but comparatively modest increase of 66 % in myofibrillar protein synthesis following nerve damage (Figure 3), while we calculated an estimated increase of 270 % in myofibrillar protein breakdown (Figure 4). As such, in our model of chronic constriction injury to the nerve the molecular signaling in skeletal muscle lines up relatively closely with the protein turnover data from the tracer experiments, showing moderately increased markers of protein synthesis and substantially increased markers of protein breakdown.



3.5 Conclusion

In summary, we found that chronic nerve constriction induced muscle loss is primarily based on muscle fiber atrophy, not the loss of muscle fibers. We measured myofibrillar FSR in muscles affected by such muscle loss and found it to be significantly increased as opposed to decreased. Supported by other recent findings, this indicates that myofibrillar FSR might be driven by muscle damage and reflects muscle remodeling rather than net protein accretion [62; 69]. Since myofibrillar FSR is increased rather than decreased, substantial muscle protein breakdown is likely to be the predominant force behind muscle loss in this model. This observation is supported by slight increases in anabolic signaling, but strong increases in catabolic signaling resembling the findings from the tracer experiments. As such, slowing myofibrillar protein breakdown appears to be the more promising target than improving an already accelerated rate of myofibrillar protein synthesis, for the development of interventions that hope to ameliorate the course of muscle wasting with chronic constriction injury to the nerve.

GRAPHICAL SUMMARY



Graphical representation of experimental design, methods and main results

Nerve damage was caused by chronic constriction injury to the sciatic nerve. Stable isotope labeling was performed through D₂O. Analysis focused on histology, immunoblotting and GC-MS. Despite apparent muscle fiber atrophy, rates of myofibrillar protein synthesis and anabolic signaling were increased, indicating that even further elevated myofibrillar protein breakdown and catabolic signaling likely account for the negative net protein balance and muscle loss seen in this model.

REFERENCES

- [1] I. Janssen, S.B. Heymsfield, Z. Wang, and R. Ross, Skeletal muscle mass and distribution in 468 men and women aged 18–88 yr. *Journal of applied physiology* 89 (2000) 81-88.
- [2] P. Webb, Energy expenditure and fat-free mass in men and women. *Am J Clin Nutr* 34 (1981) 1816-26.
- [3] B.K. Pedersen, Muscle as a secretory organ. *Comprehensive Physiology* 3 (2013) 1337-62.
- [4] E.J. Metter, L.A. Talbot, M. Schrager, and R. Conwit, Skeletal muscle strength as a predictor of all-cause mortality in healthy men. *The journals of gerontology. Series A, Biological sciences and medical sciences* 57 (2002) B359-65.
- [5] ACSM, American College of Sports Medicine position stand. The recommended quantity and quality of exercise for developing and maintaining cardiorespiratory and muscular fitness in healthy adults. *Med Sci Sports Exerc* 22 (1990) 265-74.
- [6] S. Al-Majid, and D.O. McCarthy, Cancer-induced fatigue and skeletal muscle wasting: the role of exercise. *Biological research for nursing* 2 (2001) 186-197.
- [7] S. Weber-Carstens, J. Schneider, T. Wollersheim, A. Assmann, J. Bierbrauer, A. Marg, H. Al Hasani, A. Chadt, K. Wenzel, and S. Koch, Critical illness myopathy and GLUT4: significance of insulin and muscle contraction. *American journal of respiratory and critical care medicine* 187 (2013) 387-396.
- [8] D.R. Thomas, Loss of skeletal muscle mass in aging: examining the relationship of starvation, sarcopenia and cachexia. *Clinical Nutrition* 26 (2007) 389-399.
- [9] K. Marquis, R. Debigaré, Y. Lacasse, P. LeBlanc, J. Jobin, G. Carrier, and F. Maltais, Midthigh muscle cross-sectional area is a better predictor of mortality than body mass index in patients with chronic obstructive pulmonary disease. *American Journal of Respiratory and Critical Care Medicine* 166 (2002) 809-813.
- [10] J. Springer, S. Von Haehling, and S.D. Anker, The need for a standardized definition for cachexia in chronic illness. *Nature clinical practice Endocrinology & metabolism* 2 (2006) 416-417.
- [11] S.D. Anker, P. Ponikowski, S. Varney, T.P. Chua, A.L. Clark, K.M. Webb-Peploe, D. Harrington, W.J. Kox, P.A. Poole-Wilson, and A.J. Coats, Wasting as independent risk factor for mortality in chronic heart failure. *The Lancet* 349 (1997) 1050-1053.
- [12] B.T. Wall, M.L. Dirks, and L.J. van Loon, Skeletal muscle atrophy during short-term disuse: implications for age-related sarcopenia. *Ageing research reviews* (2013).
- [13] I. Janssen, D.S. Shepard, P.T. Katzmarzyk, and R. Roubenoff, The healthcare costs of sarcopenia in the United States. *Journal of the American Geriatrics Society* 52 (2004) 80-5.
- [14] M.L. Dirks, D. Hansen, A. Van Assche, P. Dendale, and L.J. Van Loon, Neuromuscular electrical stimulation prevents muscle wasting in critically ill, comatose patients. *Clinical science (London, England : 1979)* (2014).
- [15] A.F. Baptista, J.R. Gomes, J.T. Oliveira, S.M. Santos, M.A. Vannier-Santos, and A. Martinez, High-and low-frequency transcutaneous electrical nerve stimulation delay sciatic nerve regeneration after crush lesion in the mouse. *Journal of the Peripheral Nervous System* 13 (2008) 71-80.
- [16] M.J. Rennie, H. Wackerhage, E.E. Spangenburg, and F.W. Booth, Control of the size of the human muscle mass. *Annu. Rev. Physiol.* 66 (2004) 799-828.
- [17] E. Simmons, J.D. Fluckey, and S.E. Riechman, Cumulative Muscle Protein Synthesis and Protein Intake Requirements. *Annual review of nutrition* 36 (2016) 17-43.
- [18] M.B. Reid, A.R. Judge, and S.C. Bodine, CrossTalk opposing view: The dominant mechanism causing disuse muscle atrophy is proteolysis. *The Journal of physiology* 592 (2014) 5345-5347.
- [19] P. Dyck, *Peripheral neuropathy*, Elsevier Inc., 2005.

- [20] M.A. Ahad, P.M. Fogerson, G.D. Rosen, P. Narayanaswami, and S.B. Rutkove, Electrical characteristics of rat skeletal muscle in immaturity, adulthood and after sciatic nerve injury, and their relation to muscle fiber size. *Physiological measurement* 30 (2009) 1415-27.
- [21] M. Liu, D. Zhang, C. Shao, J. Liu, F. Ding, and X. Gu, Expression pattern of myostatin in gastrocnemius muscle of rats after sciatic nerve crush injury. *Muscle & nerve* 35 (2007) 649-56.
- [22] C. Sommer, Neuropathic Pain Model, Chronic Constriction Injury. *Encyclopedia of Pain* (2013) 2072-2075.
- [23] L. Brocca, L. Toniolo, C. Reggiani, R. Bottinelli, M. Sandri, and M.A. Pellegrino, FoxO-dependent atrogenes vary among catabolic conditions and play a key role in muscle atrophy induced by hindlimb suspension. *The Journal of physiology* 595 (2017) 1143-1158.
- [24] M.J. Rennie, An introduction to the use of tracers in nutrition and metabolism. *Proceedings of the Nutrition Society* 58 (1999) 935-944.
- [25] L. Salonen, L. Kaihola, B. Carter, G.T. Cook, and C.J. Passo, Environmental liquid scintillation analysis, *Handbook of Radioactivity Analysis (Third Edition)*, Elsevier, 2012, pp. 625-693.
- [26] T.B. Coplen, Compilation of minimum and maximum isotope ratios of selected elements in naturally occurring terrestrial materials and reagents, US Department of the Interior, US Geological Survey, 2002.
- [27] S.J. Carlson-Newberry, and R.B. Costello, Emerging Technologies for Nutrition Research, NATIONAL ACADEMY OF SCIENCES WASHINGTON DC COMMITTEE ON MILITARY NUTRITION RESEARCH, 1997.
- [28] H.-J. Hübschmann, *Handbook of GC-MS: fundamentals and applications*, John Wiley & Sons, 2015.
- [29] P.J. Linstrom, and W. Mallard, NIST chemistry webbook, National Institute of Standards and Technology Gaithersburg, MD, 2001.
- [30] R. Busch, Y.K. Kim, R.A. Neese, V. Schade-Serin, M. Collins, M. Awada, J.L. Gardner, C. Beysen, M.E. Marino, L.M. Misell, and M.K. Hellerstein, Measurement of protein turnover rates by heavy water labeling of nonessential amino acids. *Biochimica et biophysica acta* 1760 (2006) 730-44.
- [31] R.R. Wolfe, and D.L. Chinkes, *Isotope tracers in metabolic research: principles and practice of kinetic analysis*, John Wiley & Sons, 2005.
- [32] H.G. Gasier, S.E. Riechman, M.P. Wiggs, S.F. Previs, and J.D. Fluckey, A comparison of $2H_2O$ and phenylalanine flooding dose to investigate muscle protein synthesis with acute exercise in rats. *American journal of physiology. Endocrinology and metabolism* 297 (2009) E252-9.
- [33] R. Ramakrishnan, Alternative equations for whole-body protein synthesis and for fractional synthetic rates of proteins. *Metabolism* 56 (2007) 1550-60.
- [34] I.-Y. Kim, S.-H. Suh, I.-K. Lee, and R.R. Wolfe, Applications of stable, nonradioactive isotope tracers in in vivo human metabolic research. *Experimental & molecular medicine* 48 (2017) e203.
- [35] H.T. Langer, J.M. Senden, A.P. Gijzen, S. Kempa, L.J. van Loon, and S. Spuler, Muscle atrophy due to nerve damage is accompanied by elevated myofibrillar protein synthesis rates. *Frontiers in Physiology* 9 (2018) 1220.
- [36] P. Wu, A. Chawla, R.J. Spinner, C. Yu, M.J. Yaszemski, A.J. Windebank, and H. Wang, Key changes in denervated muscles and their impact on regeneration and reinnervation. *Neural regeneration research* 9 (2014) 1796.
- [37] W.S. al-Ahood, D.M. Lewis, and H. Schmalbruch, Effects of chronic electrical stimulation on contractile properties of long-term denervated rat skeletal muscle. *J Physiol* 441 (1991) 243-56.
- [38] D. Goldspink, The effects of denervation on protein turnover of rat skeletal muscle. *Biochemical Journal* 156 (1976) 71-80.

- [39] D.W. West, L.M. Baehr, G.R. Marcotte, C.M. Chason, L. Tolento, A.V. Gomes, S.C. Bodine, and K. Baar, Acute resistance exercise activates rapamycin-sensitive and-insensitive mechanisms that control translational activity and capacity in skeletal muscle. *The Journal of physiology* 594 (2016) 453-468.
- [40] K. Baar, and K. Esser, Phosphorylation of p70S6k correlates with increased skeletal muscle mass following resistance exercise. *American Journal of Physiology-Cell Physiology* 276 (1999) C120-C127.
- [41] H. Escobar, V. Schowel, S. Spuler, A. Marg, and Z. Izsvak, Full-length Dysferlin Transfer by the Hyperactive Sleeping Beauty Transposase Restores Dysferlin-deficient Muscle. *Mol Ther Nucleic Acids* 5 (2016) e277.
- [42] J.E. Gilda, and A.V. Gomes, Stain-Free total protein staining is a superior loading control to β -actin for Western blots. *Analytical biochemistry* 440 (2013) 186-188.
- [43] R. Busch, Y.-K. Kim, R.A. Neese, V. Schade-Serin, M. Collins, M. Awada, J.L. Gardner, C. Beysen, M.E. Marino, and L.M. Misell, Measurement of protein turnover rates by heavy water labeling of nonessential amino acids. *Biochimica et Biophysica Acta (BBA)-General Subjects* 1760 (2006) 730-744.
- [44] T.J. Humphrey, and D.D. Davies, A sensitive method for measuring protein turnover based on the measurement of 2-3H-labelled amino acids in protein. *Biochemical Journal* 156 (1976) 561-568.
- [45] T.J. Humphrey, and D.D. Davies, A new method for the measurement of protein turnover. *Biochemical Journal* 148 (1975) 119-127.
- [46] D.J. Wilkinson, M.S. Brook, K. Smith, and P.J. Atherton, Stable isotope tracers and exercise physiology: past, present and future. *J Physiol* 595 (2017) 2873-2882.
- [47] D.J. Wilkinson, M.V. Franchi, M.S. Brook, M.V. Narici, J.P. Williams, W.K. Mitchell, N.J. Szewczyk, P.L. Greenhaff, P.J. Atherton, and K. Smith, A validation of the application of D(2)O stable isotope tracer techniques for monitoring day-to-day changes in muscle protein subfraction synthesis in humans. *American journal of physiology. Endocrinology and metabolism* 306 (2014) E571-9.
- [48] W.N. Lee, S. Bassilian, H.O. Ajie, D.A. Schoeller, J. Edmond, E.A. Bergner, and L.O. Byerley, In vivo measurement of fatty acids and cholesterol synthesis using D2O and mass isotopomer analysis. *The American journal of physiology* 266 (1994) E699-708.
- [49] N.A. Burd, D.W. West, A.W. Staples, P.J. Atherton, J.M. Baker, D.R. Moore, A.M. Holwerda, G. Parise, M.J. Rennie, and S.K. Baker, Low-load high volume resistance exercise stimulates muscle protein synthesis more than high-load low volume resistance exercise in young men. *PLoS one* 5 (2010) e12033.
- [50] E. Helander, On quantitative muscle protein determination: sarcoplasm and myofibril protein content of normal and atrophic skeletal muscles. (1957).
- [51] T.G. Sobolevsky, A.I. Revelsky, B. Miller, V. Oriedo, E.S. Chernetsova, and I.A. Revelsky, Comparison of silylation and esterification/acylation procedures in GC-MS analysis of amino acids. *Journal of separation science* 26 (2003) 1474-1478.
- [52] H.G. Gasier, J.D. Fluckey, and S.F. Previs, The application of 2H2O to measure skeletal muscle protein synthesis. *Nutrition & metabolism* 7 (2010) 31.
- [53] P.Q. Baumann, W.S. Stirewalt, B.D. O'Rourke, D. Howard, and K.S. Nair, Precursor pools of protein synthesis: a stable isotope study in a swine model. *The American journal of physiology* 267 (1994) E203-9.
- [54] L. Van Loon, Y. Boirie, A. Gijsen, J. Fauquant, A. De Roos, A. Kies, S. Lemosquet, W. Saris, and R. Koopman, The production of intrinsically labeled milk protein provides a functional tool for human nutrition research. *Journal of dairy science* 92 (2009) 4812-4822.
- [55] H.H. Huidekoper, M.T. Ackermans, R. Koopman, L.J. van Loon, H.P. Sauerwein, and F.A. Wijburg, Normal rates of whole-body fat oxidation and gluconeogenesis after overnight

- fasting and moderate-intensity exercise in patients with medium-chain acyl-CoA dehydrogenase deficiency. *Journal of inherited metabolic disease* 36 (2013) 831-40.
- [56] I.-Y. Kim, S.-H. Suh, I.-K. Lee, and R.R. Wolfe, Applications of stable, nonradioactive isotope tracers in in vivo human metabolic research. *Experimental & Molecular Medicine* 48 (2016) e203-e203.
- [57] R.R. Wolfe, and D.L. Chinkes, *Isotope tracers in metabolic research: principles and practice of kinetic analysis*, John Wiley & Sons, 2004.
- [58] D.J. Millward, P.J. Garlick, R.J. Stewart, D.O. Nnanyelugo, and J.C. Waterlow, Skeletal-muscle growth and protein turnover. *The Biochemical journal* 150 (1975) 235-43.
- [59] A.J. Hector, C. McGlory, F. Damas, N. Mazara, S.K. Baker, and S.M. Phillips, Pronounced energy restriction with elevated protein intake results in no change in proteolysis and reductions in skeletal muscle protein synthesis that are mitigated by resistance exercise. *FASEB journal : official publication of the Federation of American Societies for Experimental Biology* 32 (2018) 265-275.
- [60] M. Pietzke, C. Zasada, S. Mudrich, and S. Kempa, Decoding the dynamics of cellular metabolism and the action of 3-bromopyruvate and 2-deoxyglucose using pulsed stable isotope-resolved metabolomics. *Cancer & metabolism* 2 (2014) 1-11.
- [61] R. Nilwik, T. Snijders, M. Leenders, B.B. Groen, J. van Kranenburg, L.B. Verdijk, and L.J. van Loon, The decline in skeletal muscle mass with aging is mainly attributed to a reduction in type II muscle fiber size. *Experimental gerontology* 48 (2013) 492-8.
- [62] F. Damas, S.M. Phillips, C.A. Libardi, F.C. Vechin, M.E. Lixandrão, P.R. Jannig, L.A. Costa, A.V. Bacurau, T. Snijders, and G. Parise, Resistance training-induced changes in integrated myofibrillar protein synthesis are related to hypertrophy only after attenuation of muscle damage. *The Journal of physiology* 594 (2016) 5209-5222.
- [63] N.A. Burd, H.M. Hamer, B. Pennings, W.F. Pellikaan, J.M. Senden, A.P. Gijzen, and L.J. van Loon, Substantial differences between organ and muscle specific tracer incorporation rates in a lactating dairy cow. *PLoS One* 8 (2013) e68109.
- [64] S.M. Phillips, and C. McGlory, CrossTalk proposal: The dominant mechanism causing disuse muscle atrophy is decreased protein synthesis. *The Journal of physiology* 592 (2014) 5341-5343.
- [65] B.T. Wall, M.L. Dirks, T. Snijders, J.W. van Dijk, M. Fritsch, L.B. Verdijk, and L.J. van Loon, Short-term muscle disuse lowers myofibrillar protein synthesis rates and induces anabolic resistance to protein ingestion. *American journal of physiology. Endocrinology and metabolism* 310 (2016) E137-47.
- [66] B.T. Wall, T. Snijders, J.M. Senden, C.L. Ottenbros, A.P. Gijzen, L.B. Verdijk, and L.J. van Loon, Disuse impairs the muscle protein synthetic response to protein ingestion in healthy men. *The Journal of Clinical Endocrinology & Metabolism* 98 (2013) 4872-4881.
- [67] R. Koopman, and L.J. van Loon, Aging, exercise, and muscle protein metabolism. *J Appl Physiol* (1985) 106 (2009) 2040-8.
- [68] D.F. Goldspink, *Changes in the size and protein turnover of the soleus muscle in response to immobilization or denervation*, Portland Press Limited, 1978.
- [69] C.J. Mitchell, T.A. Churchward-Venne, D. Cameron-Smith, and S.M. Phillips, What is the relationship between the acute muscle protein synthesis response and changes in muscle mass? *J Appl Physiol* (1985) 118 (2015) 495-7.
- [70] K.D. Tipton, D.L. Hamilton, and I.J. Gallagher, Assessing the Role of Muscle Protein Breakdown in Response to Nutrition and Exercise in Humans. *Sports Medicine* (2018) 1-12.
- [71] R.A. Saxton, and D.M. Sabatini, mTOR signaling in growth, metabolism, and disease. *Cell* 168 (2017) 960-976.

- [72] S.C. Bodine, and L.M. Baehr, Skeletal muscle atrophy and the E3 ubiquitin ligases MuRF1 and MAFbx/atrogen-1. *American Journal of Physiology-Endocrinology and Metabolism* 307 (2014) E469-E484.
- [73] R. Ogasawara, K. Kobayashi, A. Tsutaki, K. Lee, T. Abe, S. Fujita, K. Nakazato, and N. Ishii, mTOR signaling response to resistance exercise is altered by chronic resistance training and detraining in skeletal muscle. *Journal of Applied Physiology* 114 (2013) 934-940.
- [74] S.C. Bodine, T.N. Stitt, M. Gonzalez, W.O. Kline, G.L. Stover, R. Bauerlein, E. Zlotchenko, A. Scrimgeour, J.C. Lawrence, D.J. Glass, and G.D. Yancopoulos, Akt/mTOR pathway is a crucial regulator of skeletal muscle hypertrophy and can prevent muscle atrophy in vivo. *Nat Cell Biol* 3 (2001) 1014-9.
- [75] M. Norrby, K. Evertsson, A.-K. Fjällström, A. Svensson, and S. Tågerud, Akt (protein kinase B) isoform phosphorylation and signaling downstream of mTOR (mammalian target of rapamycin) in denervated atrophic and hypertrophic mouse skeletal muscle. *J Mol Signal* 7 (2012) 7-7.
- [76] L.M. Baehr, D.W. West, A.G. Marshall, G.R. Marcotte, K. Baar, and S.C. Bodine, Muscle-specific and age-related changes in protein synthesis and protein degradation in response to hindlimb unloading in rats. *Journal of Applied Physiology* 122 (2017) 1336-1350.

AFFIDAVIT

„Ich, Henning Tim Langer, versichere an Eides statt durch meine eigenhändige Unterschrift, dass ich die vorgelegte Dissertation mit dem Thema: „The effect of chronic constriction injury to the sciatic nerve on myofibrillar protein synthesis in rat tibialis anterior“ selbstständig und ohne nicht offengelegte Hilfe Dritter verfasst und keine anderen als die angegebenen Quellen und Hilfsmittel genutzt habe. Alle Stellen, die wörtlich oder dem Sinne nach auf Publikationen oder Vorträgen anderer Autoren beruhen, sind als solche in korrekter Zitierung (siehe „Uniform Requirements for Manuscripts (URM)“ des ICMJE -www.icmje.org) kenntlich gemacht. Die Abschnitte zu Methodik (insbesondere praktische Arbeiten, Laborbestimmungen, statistische Aufarbeitung) und Resultaten (insbesondere Abbildungen, Graphiken und Tabellen) entsprechen den URM (s.o.) und werden von mir verantwortet. Mein Anteil an der ausgewählten Publikation entspricht dem, der in der untenstehenden gemeinsamen Erklärung mit dem/der Betreuer/in, angegeben ist. Sämtliche Publikationen, die aus dieser Dissertation hervorgegangen sind und bei denen ich Autor bin, entsprechen den URM (s.o.) und werden von mir verantwortet. Die Bedeutung dieser eidesstattlichen Versicherung und die strafrechtlichen Folgen einer unwahren eidesstattlichen Versicherung (§156,161 des Strafgesetzbuches) sind mir bekannt und bewusst.“

Datum und Unterschrift

AUTHOR CONTRIBUTIONS

Henning Tim Langer contributed to the following, published article:

“Muscle Atrophy Due to Nerve Damage Is Accompanied by Elevated Myofibrillar Protein Synthesis Rates”

Henning T. Langer, Joan M. G. Senden, Annemie P. Gijzen, Stefan Kempa, Luc J. C. van Loon and Simone Spuler.

Contribution: Henning Tim Langer was responsible for the design of the study, conduction of the animal experiments, collection of the samples, processing of the samples and analysis of the data (GC-MS, histochemistry, immunoblotting). All tables, figures and graphs in this publication were created by H.T. Langer and are based on original data he collected. H.T. Langer wrote the manuscript with helpful advice from Simone Spuler and Luc J.C. van Loon.

Unterschrift, Datum und Stempel des betreuenden Hochschullehrers/der betreuenden Hochschullehrerin

JOURNAL SUMMARY LIST

Journal Data Filtered By: **Selected JCR Year: 2016** Selected Editions: SCIE,SSCI
 Selected Categories: **"PHYSIOLOGY"** Selected Category Scheme: WoS
Gesamtanzahl: 84 Journale

Rank	Full Journal Title	Total Cites	Journal Impact Factor	Eigenfactor Score
1	PHYSIOLOGICAL REVIEWS	25,952	27.312	0.033220
2	Annual Review of Physiology	8,818	11.115	0.012360
3	JOURNAL OF PINEAL RESEARCH	7,278	10.391	0.008040
4	Comprehensive Physiology	2,641	6.949	0.012280
5	PHYSIOLOGY	2,946	6.076	0.006070
6	CELLULAR PHYSIOLOGY AND BIOCHEMISTRY	8,744	5.104	0.014190
7	Acta Physiologica	3,911	4.867	0.009770
8	Reviews of Physiology Biochemistry and Pharmacology	713	4.769	0.000630
9	JOURNAL OF PHYSIOLOGY-LONDON	48,567	4.739	0.047830
10	EXERCISE AND SPORT SCIENCES REVIEWS	2,674	4.431	0.003780
11	International Journal of Behavioral Nutrition and Physical Activity	7,028	4.396	0.020720
12	AMERICAN JOURNAL OF PHYSIOLOGY-LUNG CELLULAR AND MOLECULAR PHYSIOLOGY	13,082	4.281	0.018040
13	JOURNAL OF GENERAL PHYSIOLOGY	7,714	4.200	0.009920
14	AMERICAN JOURNAL OF PHYSIOLOGY-ENDOCRINOLOGY AND METABOLISM	20,249	4.142	0.025980
15	Frontiers in Physiology	7,664	4.134	0.031330
16	JOURNAL OF CELLULAR PHYSIOLOGY	17,632	4.080	0.023490
17	AMERICAN JOURNAL OF PHYSIOLOGY-RENAL PHYSIOLOGY	16,787	3.611	0.022770
18	AMERICAN JOURNAL OF PHYSIOLOGY-CELL PHYSIOLOGY	16,627	3.602	0.019200
19	JOURNAL OF BIOLOGICAL RHYTHMS	2,617	3.500	0.004220
20	AMERICAN JOURNAL OF PHYSIOLOGY-GASTROINTESTINAL AND LIVER PHYSIOLOGY	14,393	3.468	0.020340
21	JOURNAL OF APPLIED PHYSIOLOGY	42,740	3.351	0.030480



Muscle Atrophy Due to Nerve Damage Is Accompanied by Elevated Myofibrillar Protein Synthesis Rates

Henning T. Langer^{1,2,3*}, Joan M. G. Senden⁴, Annemie P. Gijzen⁴, Stefan Kempa^{5,6}, Luc J. C. van Loon⁴ and Simone Spuler^{1,2,3,5,6}

¹ Experimental and Clinical Research Center, a Joint Cooperation of Max Delbrück Center for Molecular Medicine and Charité – Universitätsmedizin Berlin, Berlin, Germany, ² Berlin-Brandenburg Center for Regenerative Therapies, Charité – Universitätsmedizin Berlin, Berlin, Germany, ³ Charité – Universitätsmedizin Berlin, Berlin, Germany, ⁴ Department of Human Biology, NUTRIM School of Nutrition and Translational Research in Metabolism, Maastricht University Medical Centre+, Maastricht, Netherlands, ⁵ Berlin Institute of Health, Berlin, Germany, ⁶ Max Delbrück Center for Molecular Medicine in the Helmholtz Association, Berlin, Germany

OPEN ACCESS

Edited by:

Susan V. Brooks,
University of Michigan, United States

Reviewed by:

Kunihiro Sakuma,
Tokyo Institute of Technology, Japan
Julien Ochala,
King's College London,
United Kingdom

*Correspondence:

Henning T. Langer
htlanger@ucdavis.edu

Specialty section:

This article was submitted to
Striated Muscle Physiology,
a section of the journal
Frontiers in Physiology

Received: 22 June 2018

Accepted: 13 August 2018

Published: 31 August 2018

Citation:

Langer HT, Senden JMG, Gijzen AP, Kempa S, van Loon LJC and Spuler S (2018) Muscle Atrophy Due to Nerve Damage Is Accompanied by Elevated Myofibrillar Protein Synthesis Rates. *Front. Physiol.* 9:1220. doi: 10.3389/fphys.2018.01220

Muscle loss is a severe complication of many medical conditions such as cancer, cardiac failure, muscular dystrophies, and nerve damage. The contribution of myofibrillar protein synthesis (MPS) to the loss of muscle mass after nerve damage is not clear. Using deuterium oxide (D₂O) labeling, we demonstrate that MPS is significantly increased in rat *m. tibialis anterior* (TA) compared to control (3.23 ± 0.72 [damaged] to $2.09 \pm 0.26\% \cdot \text{day}^{-1}$ [control]) after 4 weeks of nerve constriction injury. This is the case despite substantial loss of mass of the TA (350 ± 96 mg [damaged] to 946 ± 361 mg [control]). We also show that expression of regulatory proteins involved with MPS (p70s6k1: 2.4 ± 0.3 AU [damaged] to 1.8 ± 0.2 AU [control]) and muscle protein breakdown (MPB) (MAFbx: 5.3 ± 1.2 AU [damaged] to 1.4 ± 0.4 AU [control]) are increased in nerve damaged muscle. Furthermore, the expression of p70s6k1 correlates with MPS rates ($r^2 = 0.57$). In conclusion, this study shows that severe muscle wasting following nerve damage is accompanied by increased as opposed to decreased MPS.

Keywords: skeletal muscle, atrophy, muscle loss, myofibrillar, protein synthesis, nerve damage, stable isotope, deuterium oxide

INTRODUCTION

Skeletal muscle is the biggest organ of the human body, comprising at least 40% of its mass and containing 50–75% of all body proteins (Frontera and Ochala, 2015). It is pivotal to health and locomotion, and the lack of muscle mass and strength is associated with severely reduced independence, quality of life, and life expectancy (Metter et al., 2002; Wannamethee et al., 2007). Many clinical conditions are accompanied by muscle loss, such as cancer, COPD, or heart failure (Rosenberg, 1997; Al-Majid and McCarthy, 2001; Marquis et al., 2002; Thomas, 2007). Currently, no drug treatment for muscle wasting is available, with exercise and ample protein intake being the only *bona fide* intervention to slow muscle loss (Sepulveda et al., 2015; Garber, 2016). However, there are situations of muscle loss where physical activity is not an option. Such as in patients with fractures, critically ill patients or nerve damage. Peripheral nerve damage is a frequently occurring clinical condition that can be caused by disease or trauma (Dyck, 2005). A common model to study peripheral nerve damage is chronic constriction injury to the nerve (Bennett and Xie, 1988). Chronic constriction injury to the nerve is accompanied by debilitating symptoms

such as neuropathic pain, hampered motor function and skeletal muscle atrophy (Bennett and Xie, 1988). Even though nerve function may recover, this is often outlasted by the deteriorating effects on muscle tissue. Although chronic nerve constriction is well investigated in respect to its implications for pain in animals, very little is known on the physiology of muscle wasting.

Muscle mass is determined by the balance between muscle protein synthesis (MPS) and muscle protein breakdown (MPB). Either side of the balance may be disturbed. Consequently, most muscle atrophies are assumed to show a combination of decreased MPS and increased MPB (McKinnell and Rudnicki, 2004). Yet, the individual contribution of decreased MPS may differ between various types of atrophies. For example in disuse atrophy in humans, blunted MPS rates seem to be the predominant cause for a decline in muscle mass (Wall et al., 2013a,b, 2016). Similarly, decreased MPS has been reported for starvation, sarcopenia, cachexia, and other conditions of muscle wasting, indicating a potential benefit of interventions which increase MPS (Emery et al., 1984; Yarasheski et al., 1993; Hector et al., 2018). In nerve damage induced atrophy, early work has suggested varying effects of denervation on MPS. Depending on the time point, decreased as well as transiently increased MPS rates were found in very young rats after nerve transection (Goldspink, 1976, 1978; Goldspink et al., 1983). How MPS rates are affected by chronic nerve constriction in adult animals is not known. Furthermore, previous studies using stable isotope labeling with the flooding dose- or primed continuous infusion technique were restricted to an MPS assessment period of a few hours, reducing their ability to predict absolute changes in muscle mass (Mitchell et al., 2014; Reid et al., 2014). The reemergence of deuterium oxide (D₂O) as a mean to study integrated MPS *in vivo* over multiple days- or weeks, however, offers an attractive solution for this problem (Busch et al., 2006; Wilkinson et al., 2014; Damas et al., 2016).

Therefore we set out to investigate the effects of chronic nerve constriction on MPS. We combined long term D₂O-mediated tracer experiments in adult rats with absolute changes in muscle mass, immunohistochemical analysis and protein expression data. We hypothesized that nerve constriction would cause a decrease in MPS rates. However, we found that despite substantial muscle loss, nerve damage induced atrophy is accompanied by chronically elevated as opposed to reduced myofibrillar protein synthesis (MPS) rates.

MATERIALS AND METHODS

Ethical Approval and Animal Experiments

The animal experiments were approved by the local authority (Landesamt für Gesundheit und Soziales, Berlin, Germany) under the reference G 0083/15 and performed at the animal care unit of the Max Delbrück Center for Molecular Medicine (MDC, Berlin).

Nerve-Damage Model

Ten male Sprague-Dawley rats [CrI:CD (SD), Charles River, Sulzfeld, Germany] between 20–21 weeks of age were housed

in individual cages. The animals were fed a diet of 20 g chow (ssniff Spezialdiäten GmbH, Soest, Germany) (**Supplementary Figure 1**) equivalent to 79 kcal*day⁻¹ to slow down commonly occurring weight gain. Nerve damage was induced via chronic constriction injury to the sciatic nerve (Sommer, 2013). The rats were anesthetized via isoflurane inhalation (~2.5%) and treated with an injection of 4–5 mg carprofen *kg⁻¹ bodyweight to reduce postsurgical pain. An incision was made along the femur, and the *vastus lateralis* was disconnected from the *biceps femoris* by blunt dissection. The sciatic nerve was exposed above the point of trifurcation and constriction injury was induced by implanting a cuff around the nerve. To further reduce postsurgical pain of the animals, they received 100 mg *kg⁻¹ metamizole. For the last 2 weeks, the animals were electrostimulated twice a week to maintain the nerve injury and impair recovery, as has been described previously (Baptista et al., 2008; Gigo-Benato et al., 2010). The animals were dissected 4 weeks post surgery, between the age of 24 and 25 weeks. In a fasted state, the animals were put under deep anesthesia via isoflurane inhalation (~3.5%) and the TA and *extensor digitorum longus* (EDL) were collected. Muscles were quickly weighed and cut in half, with one part being immediately snap frozen in liquid nitrogen and the other part being embedded in gum tragacanth for histological analysis and frozen in isopentane.

D₂O Labeling Protocol

We used a labeling protocol suitable to detect deuterium (²H) enrichments in alanine of the myofibrillar protein fraction of skeletal muscle via GC-MS similar to what has been published previously (Busch et al., 2006; Gasier et al., 2009). Briefly, 2 weeks after surgery the animals received an intraperitoneal injection of 0.014 mL *g⁻¹ bodyweight of D₂O (99.8%+ Atom D, Euriso-Top GmbH Saarbrücken) and 0.9% NaCl. This injection primed the animals and enriched their body water levels to approximately 2.5% D₂O. To maintain the label concentration, the rats received drinking water with 4% ²H₂O enrichment.

Myofibrillar Protein Extraction

Myofibrillar protein isolation was performed as described previously (Burd et al., 2012). Briefly, 80–120 mg muscle sample of rat TA (*n* = 10) was weighed into an Eppendorf tube and stored on ice. A standard buffer solution was added to each sample at 10 μL *mg⁻¹ and the muscle tissue was thoroughly homogenized. Scissors were used to mince the tissue before subsequent homogenization by plastic pestles. To fractionate a pellet rich in myofibrillar- and other structural proteins, the sample was spun at 700 g for 10 min at 4°C. The remaining pellet was washed twice with buffer and dH₂O, the supernatant was discarded and 1 mL 0.3 NaOH was added to the pellet to further solubilize the myofibrillar proteins and isolate them from collagen. The samples were heated at 50°C for 30 min. Subsequently the sample was spun at 10,000 g for 5 min at 4°C and the supernatant containing the myofibrillar protein was transferred into 4 mL screw-cap glass vials. One milliliter of 1M PCA was added to each glass vial to denature the remaining proteins. After centrifugation, the supernatant was removed and the pellet washed twice with 500 μL 70% EtOH. After removal

of the EtOH, 1.5 mL of 6M HCL was added to hydrolyze the samples over night at 110°C. The next day the samples were put in a heating block (120°C) and dried under a nitrogen steam. To further purify the amino acids, the samples were passed through Dowex exchange resin (AG 50W-X8 Resin, Bio-Rad) prior to derivatization. After purification, the glass vials were carefully vortexed and put under a nitrogen steam to dry before derivatization. Samples containing the free amino acids of the myofibrillar protein fraction were then converted to their tert-butyl dimethylsilyl (TBDMS) derivatives via the addition of 50 µL of N-tert-Butyldimethylsilyl-N-methyltrifluoroacetamide (MTBSTFA) and 50 µL of acetonitrile to the sample. Each sample was then incubated for 1 h at 70°C. The sample was then transferred to 2 mL screw-cap chromacol vials (Thermo Fisher Scientific, Schwerte, Germany) suitable for GC-MS injection.

Plasma Protein Extraction

To precipitate plasma protein, 40 µL perchloric acid (20%) were added to 360 µL plasma sample. After vortexing, free amino acids were separated from protein bound amino acids by centrifugation (3500 rpm, 20 min, 4°C). The pellet was collected and washed three times with 1 mL perchloric acid (2%) before being hydrolyzed over night as described above. After hydrolysis, samples were purified and processed for GC-MS injection as described above. Values of unlabeled samples were used as a baseline control for ²H enrichment in plasma protein bound alanine.

Free Alanine Enrichments in Plasma

Plasma samples were thawed on ice and dry 5-sulfosalicylic acid was added to the sample to deproteinize it as described previously (Trommelen et al., 2016). After vortexing, the sample was spun at 1000 g for 15 min. The supernatant was collected and then purified, processed and measured on the GC-MS as described in the sections above.

GCMS Measurement and Stable Isotope Enrichment Analysis

The alanine enrichment was determined by electron ionization gas chromatography-mass spectrometry (GC-MS; Agilent 6890N GC/5973N MSD) using selected ion monitoring of masses 232, 233, 234, 235, and 236 for their unlabeled and labeled H₂-alanine. We applied standard regression curves to assess linearity of the mass spectrometer and to control for the loss of tracer.

Immunoblotting

Approximately 400 µm of sample was cut from the histology block and homogenized in a standard lysing buffer using a pestle. Protein concentrations in the samples were determined using a bicinchoninic acid assay (BCA) kit (Thermo Fisher Scientific, Schwerte, Germany). The required volume for 40 µg of protein per sample was calculated, aliquoted and SDSPP (6×) and SDSPP in H₂O (1×) were added for a total volume of 15 µL. Commercial SDS gels (Invitrogen NuPAGE Bis-Tris Gel, Thermo Fisher Scientific, Schwerte, Germany) and electrophoresis (130–200 V)

were used to separate the proteins in each sample. The semi-dry blot technique was used for transfer (45 min at 18 V). Membranes were blocked in TBS-T (4% milk powder) for 1 h at room temperature. Membranes were then incubated with the first antibody in TBS-T (4% milk powder) or BSA overnight (**Supplementary Figure 9**). The next day, samples were washed in TBS-T and the second antibody was added for 60 min at room temperature. After washing, chemiluminescence (ECL) was used for development of the bands. Expression levels of the protein bands of interest were directly analyzed using Image Studio Lite (LI-Cor, Lincoln, NE, United States). Protein loading and transfer was controlled for with a ponceau s staining (**Supplementary Figure 2**).

Histochemistry and Immunofluorescence

Gomori trichrome and toluidine blue ATPase stainings were performed according to an established protocol (Engel and Cunningham, 1963; Ogilvie and Feedback, 1990). For the fiber type distribution, as many fibers per slice were measured as clearly distinguishable by the toluidine blue staining. For type 2 fibers this was approximately 50 per slide, for the far less abundant type 1 fibers approximately 10.

For immunofluorescence staining, freshly cut cryosections were left 1 h at RT to dry and then fixated in 3.7% paraformaldehyde. Subsequently, sections were washed and blocked in 3% BSA/PBS. Afterward sections were incubated with anti-GLUT4 antibody (**Supplementary Figure 9**), CT-3,-3/5; 1:1000 in PBS (1% BSA) for 1 h at room temperature. The sections were incubated with biotin anti rabbit (1:200) in PBS and Streptavidin-Cy3 (1:200). Nuclei were visualized with Hoechst (1:1000 in PBS) before being mounted on slides using Aqua Mount (Thermo Fisher Scientific, Schwerte, Germany).

Pictures were acquired using a Zeiss LSM 700 confocal microscope (Zeiss, Jena, Germany) and the associated vendor software Zen 2012. Mosaic pictures of the TA were created with a Leica DFC 420 microscope (Leica Microsystems, Wetzlar, Germany). Fiber number was analyzed by counting every single fiber of the section.

Body Composition Analysis

Body composition was measured using the Minispec LF90 II time domain NMR analyzer (6.5 mHz, Bruker Optics, United States). Rats were placed into a restraint tube and inserted into the instrument which measured fat mass, fat-free mass, and fluid content of the animal.

Fractional Synthesis Rate Calculations

Myofibrillar protein synthesis rates were calculated using the precursor-product method (Wall et al., 2013b).

$$\text{FSR} (\% \cdot \text{d}^{-1}) = (\Delta \text{MPE}_{\text{myo}} / (\Delta \text{MPE}_{\text{plasma}} \cdot t)) \cdot 100$$

where FSR is the fractional synthesis rate of myofibrillar proteins, $\Delta \text{MPE}_{\text{myo}}$ is the change in enrichment of ²H in muscle protein-bound alanine, $\Delta \text{MPE}_{\text{plasma}}$ is the change in enrichment of ²H in alanine found in plasma and t is time.

Statistics

Statistical tests were applied as appropriate depending on the sample- and group number. Data are expressed as scatter dot plot with the line indicating the mean, mean \pm standard deviation or floating bars (minimum to maximal value) with the line indicating the mean. After testing for normality of the data, Student's *t*-test or ANOVA with Tukey's *post hoc* test were applied depending on the number of groups. *p*-Values below 0.05 were deemed significant.

RESULTS

Nerve Damage Induces Substantial Muscle Loss

We induced sciatic nerve damage in otherwise healthy, male SD rats. We observed a fully developed muscle wasting phenotype at 28 days post surgery (Figures 1A–D). Immediately after surgery, the animals showed signs of decreased innervation of the hind limb affected, as expected after peripheral nerve injury (Gigo-Benato et al., 2010). The animals did not show any symptoms of decreased alertness or daily activity. Sciatic nerve innervated muscles lost significant mass: After 28 days TA mass had decreased by 66%, from 946 to 350 mg (Figure 1B), EDL by 50% from 264 to 132 mg (Figure 1C). In the *m. soleus* (SOL), loss of mass was less pronounced. Muscle weight decreased from 252 to 156 mg which approximates a 38% loss in muscle mass (Figure 1D). Since the SOL is almost exclusively composed of type 1 fibers (Gregory et al., 2001), this might hint toward a predominant type 2 fiber atrophy in association with disuse, rather than neurogenic atrophy. We followed this up via histological analysis.

Fiber Atrophy and Deteriorated Body Composition

Histological analysis at day 28 after initiation of nerve damage revealed signs of necrotizing myopathy with regenerating fibers, fibers with centrally located nuclei, necrotic, and atrophic fibers (Figure 2A). The Feret's diameter ranged from 43–51 μm in healthy type 1 fibers, and from 30–37 μm in damaged type 1 fibers (Figure 2B). In type 2a fibers, Feret's diameter ranged from 43–53 μm in healthy muscle and 28–47 μm in damaged muscle (Figure 2B). Type 2b fibers ranged from 52–63 μm in healthy, and 29–43 μm in damaged muscle (Figure 2B). Overall, nerve damage induced a decrease in fiber diameter in all three fiber types (Figure 2B). In our study the type 2b fibers were most affected, decreasing by 41% (\pm 13%) in Feret's diameter (Figure 2B). When type 2a and -b fibers were clustered, the loss of fiber diameter was greater than in type 1 fibers (Supplementary Figure 3). This confirms that the loss of muscle mass is predominantly based on type 2 fiber atrophy and explains why the SOL showed the least decline in muscle mass, being composed almost exclusively of type 1 fibers (Gregory et al., 2001). The total number of fibers in a complete cross section of TA from control and nerve damaged muscle were counted. In healthy muscle we found 13980 ± 999 compared to 13270 ± 652

fibers in damaged muscle (Figure 2C). These data indicate that muscular atrophy was due to loss of mass in individual fibers rather than reduction of total number of fibers, all consistent with muscular atrophy rather than dystrophy.

We asked whether sciatic nerve-induced atrophy resulted in overall changes in body composition. From day 0 to 28 days post surgery, we detected a 3.7% (\pm 1.3%) decrease in lean body mass from 75.4% (\pm 2.3%) to 71.7% (\pm 2.9%) (Figure 2D). The loss of lean body mass percentage occurred despite a tendency toward an increase in bodyweight ($p = 0.61$; Supplementary Figure 7). The decrease in lean body mass was accompanied by a slight increase in body fat percentage (Figure 2D).

Increased Myofibrillar Protein Synthesis in Atrophic Muscle

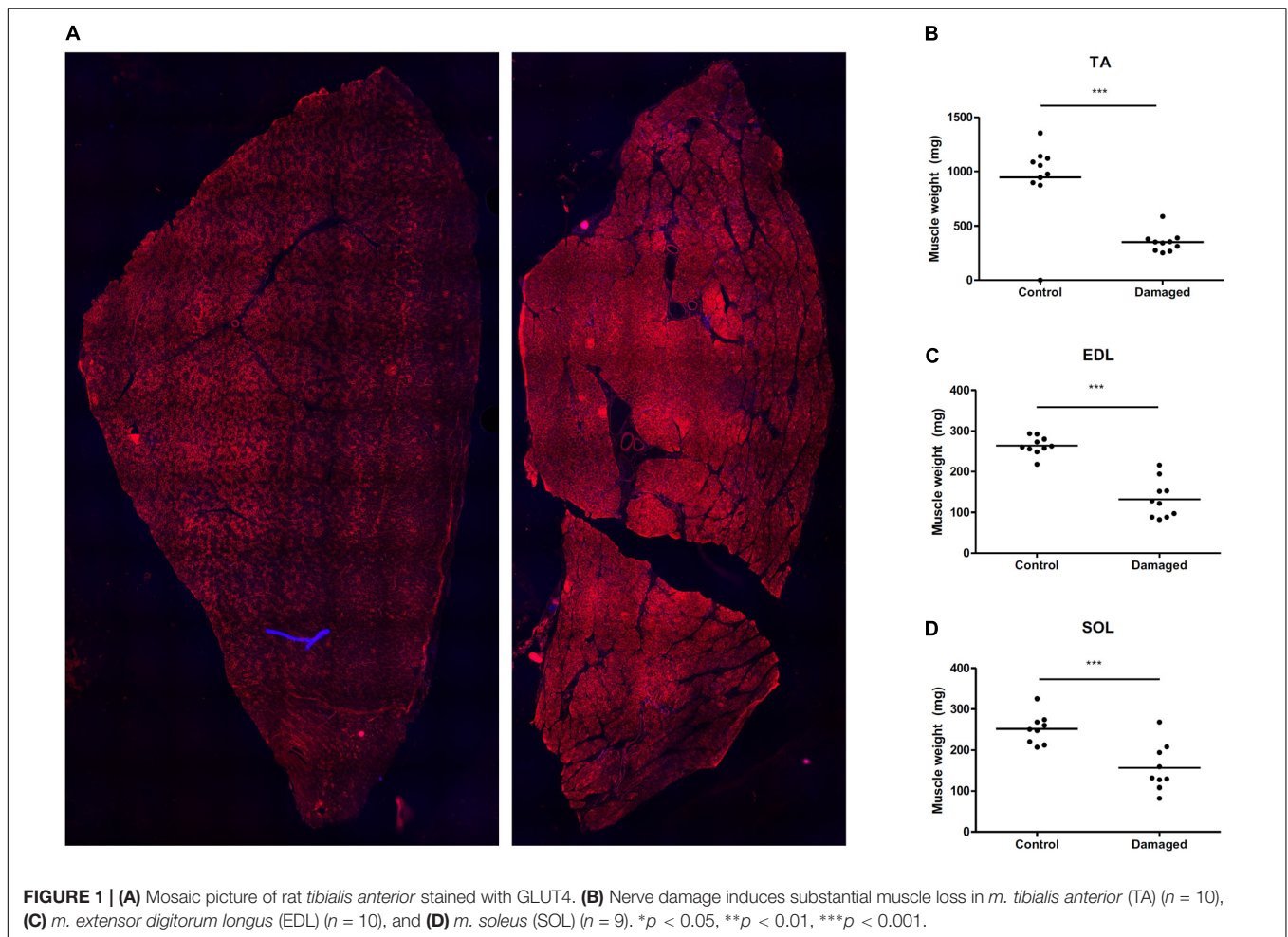
Deuterium oxide was injected and then added to regular water supply to analyze myofibrillar fractional synthetic rate (Figure 3A). We confirmed our ability to reliably detect ^2H labeled alanine in a vast amount of different rat muscle samples, obtained from several interventions which have utilized D_2O (Figure 3B). Myofibrillar fractional synthetic rate was increased 1.6-fold in the damaged compared to the control leg after 2 weeks of D_2O treatment (3.23 ± 0.72 to $2.09 \pm 0.26\% \cdot \text{day}^{-1}$, respectively) (Figure 4). Every single animal ($n = 10$) showed increased muscle protein synthesis rates in the damaged compared to the control leg (Supplementary Figure 4). To our knowledge, this is the first study showing an integrated increase in MPS during a prolonged period of loss of muscle mass.

Expression of Key Signaling Proteins Regulating Muscle Size

Skeletal muscle proteolysis is partially regulated by the E3 ubiquitin proteasome pathway and its muscle specific ligases MAFbx and MuRF1 (Bodine et al., 2001). To investigate how key signaling proteins of the proteasome pathway are regulated in our model, we investigated MAFbx and MuRF1 by Western blot analysis. Expression of MAFbx was increased fourfold in the damaged versus the control leg (5.3 ± 1.2 to 1.4 ± 0.4 AU, respectively) (Figure 5A, upper panel). MuRF1 expression followed a similar pattern ($p < 0.0001$) (Supplementary Figure 5). Protein expression of p70s6k1 increased 1.4-fold in the damaged leg (2.4 ± 0.3 to 1.8 ± 0.2 AU) (Figure 5A, lower panel). Phosphorylated p70s6k1 could not be detected (Supplementary Figure 6). We found a correlation between p70s6k1 expression and myofibrillar fractional synthesis rates ($r^2 = 0.57$) (Figure 6A). The correlation for p70s6k1 and FSR is independent of the intervention effect and still present if the analysis is restricted to the control leg ($r^2 = 0.65$) (Supplementary Figure 8).

DISCUSSION

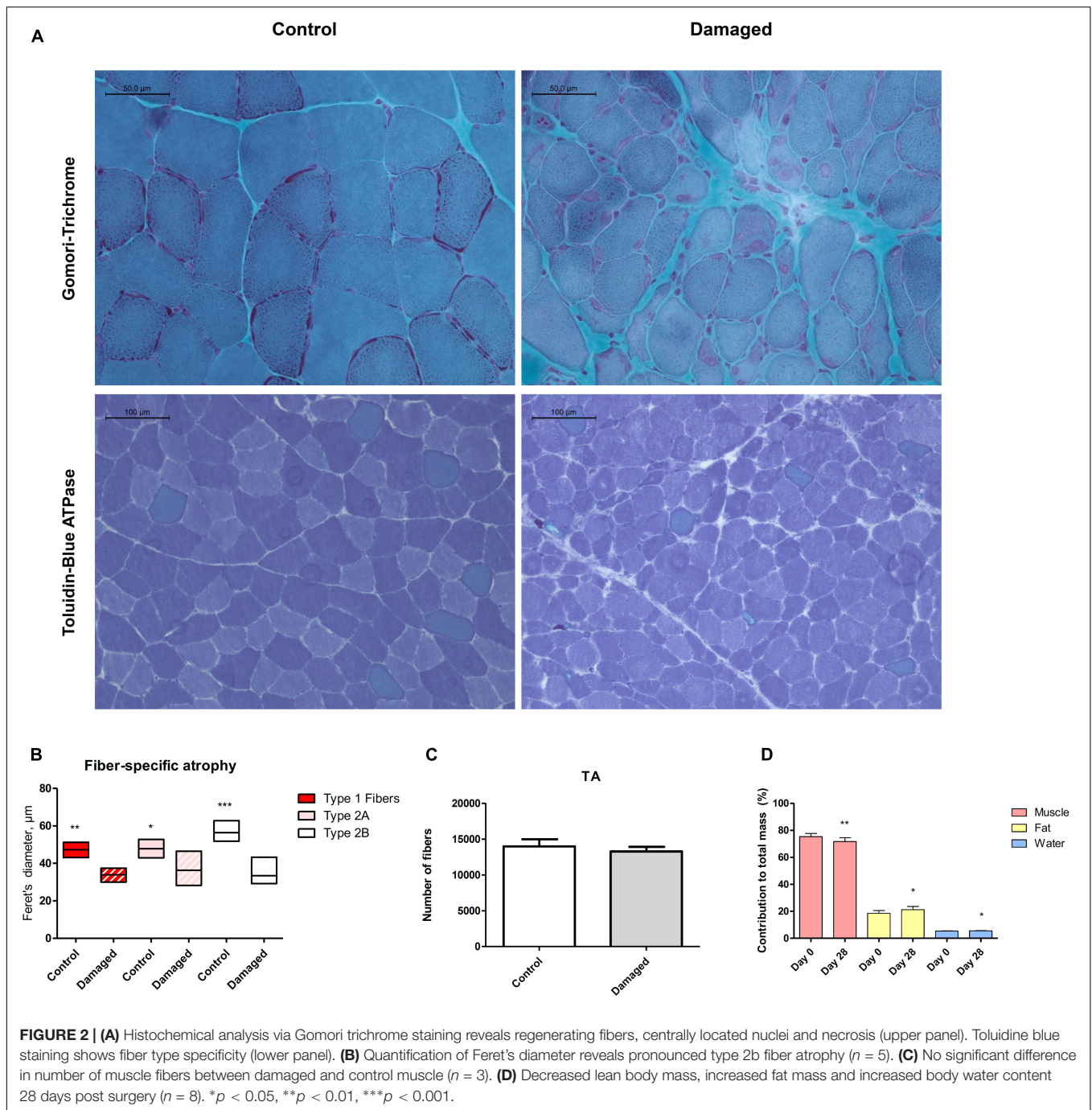
The most prevalent assumption is that in most situations of muscle loss, there is a decrease in protein synthesis as well an increase in protein breakdown (McKinnell and Rudnicki, 2004). In disuse atrophy and immobilization in humans, a decrease in MPS appears to be the predominant mechanism causing



muscle loss (Wall et al., 2013a; Phillips and McGlory, 2014). A decrease in MPS has also been observed for diet induced muscle atrophy in obese men, cancer cachexia, sepsis, and burned patients (Emery et al., 1984; Sakurai et al., 1995; Lang et al., 2007; Hector et al., 2018). In our study, we investigated chronic changes in MPS in response to nerve damage induced muscle atrophy. In stark contrast to the scenarios mentioned above, we found that MPS rates are increased as opposed to decreased during nerve damage induced muscle loss (Figure 4). Early studies on MPS after nerve damage have found varying results. MPS was reported to be transiently increased *in vitro* and *in vivo* by Buse, Goldspink and others (Buse et al., 1965; Goldspink, 1976, 1978). Later work has shown a decrease in MPS in muscle that has undergone compensatory growth with subsequent nerve transection (Goldspink et al., 1983). However, the implications of these studies differ profoundly from our findings. One reason are the differences between the nerve damage models: while a lot of work has been done on nerve transection, less is known for chronic constriction injuries to the nerve, which was the model in this study. In fact, no study thus far had investigated how muscle protein turnover and MPS are affected by nerve constriction injury. Furthermore, the studies finding an increase in tracer incorporation into the EDL and SOL after nerve transection were

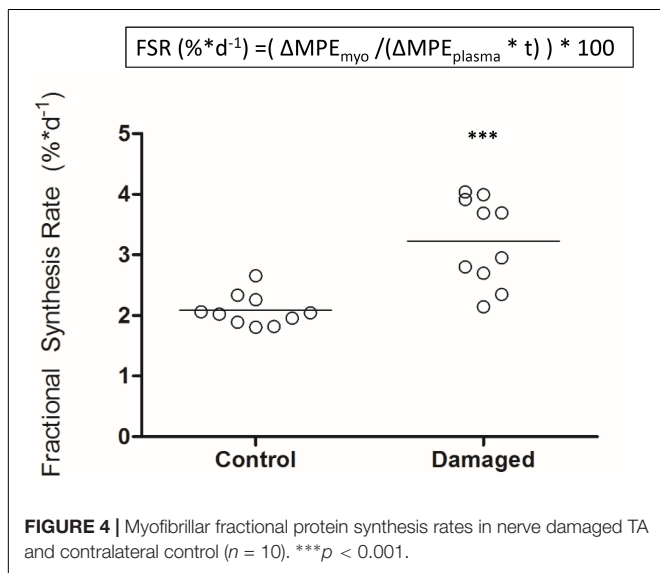
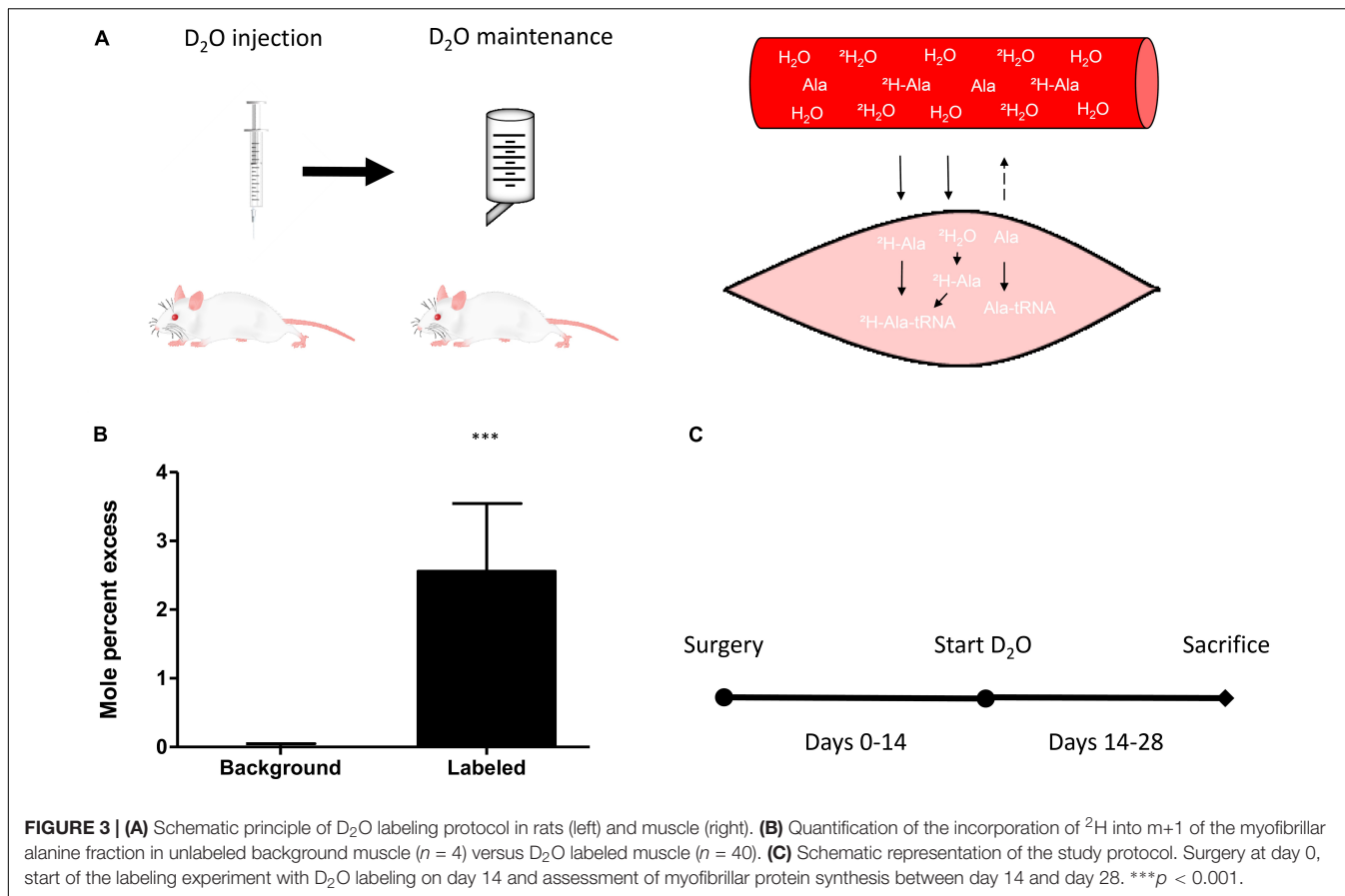
performed in particularly young rats (Goldspink, 1976, 1978). Undergoing age related growth, these animals still increased absolute mass of the denervated muscle over the course of the experiment (Goldspink, 1976, 1978). The result was slowed growth and relative atrophy of the affected muscles compared to control animals rather than absolute atrophy. In the face of a systemically anabolic environment, increased MPS rates may be less surprising. We chose full grown, adult rats (21–22 weeks old) and controlled their food intake to avoid excess bodyweight- and associated muscle gains (Supplementary Figure 7). Over the course of 4 weeks after the surgery our animals lost 66% of the TA compared to the contralateral control leg, and 50% of the EDL mass, respectively (Figures 1B,C). Despite this significant decrease in muscle mass we found a 1.6-fold increase in MPS in the TA (Figure 4). To our knowledge, this is the first study finding such a pronounced increase in integrated MPS despite absolute atrophy of the muscle. This supports the notion that MPS rates may be more indicative of muscle remodeling and ongoing regeneration than muscle growth *per se* (Ochala et al., 2011; Mitchell et al., 2014; Damas et al., 2016).

The timing to assess muscle protein turnover is crucial to the understanding of the changes in muscle mass. It is well known that the time course of muscle protein turnover in response to



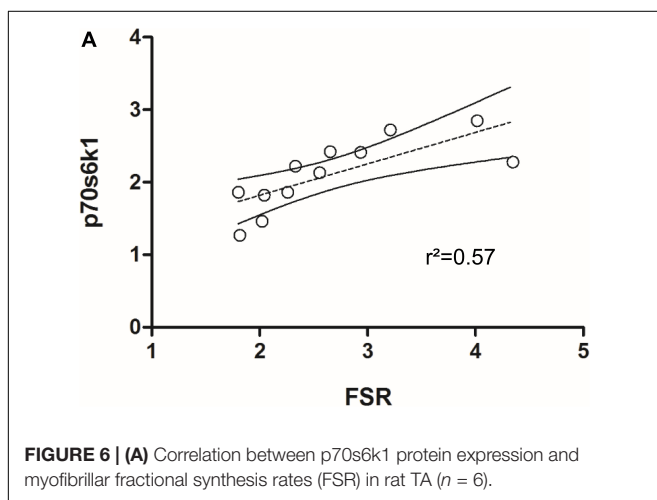
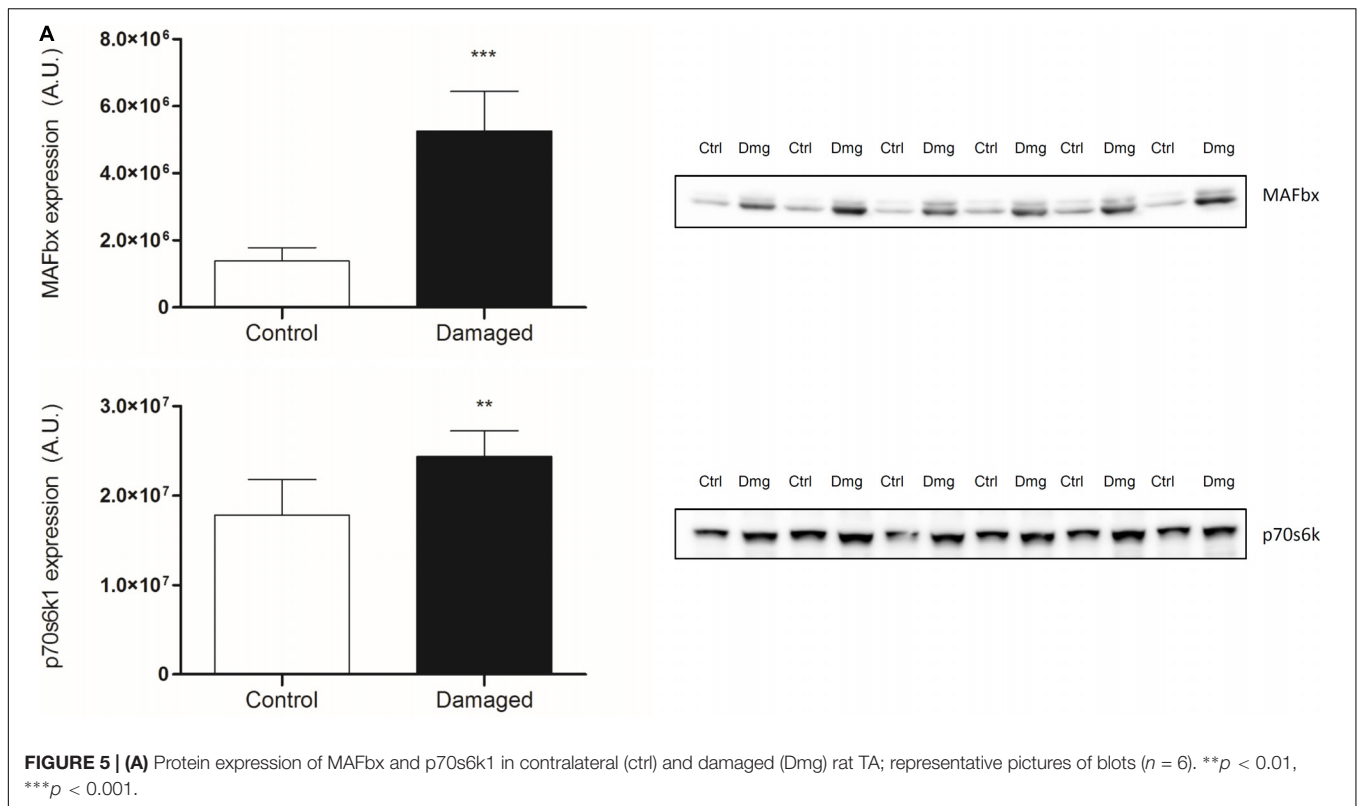
an atrophic stimulus is dynamic and depends on a variety of parameters. For example in muscle disuse atrophy, the majority of the changes to muscle protein turnover occur within the first week after the onset of the stimulus (Wall et al., 2016). It is thought that MPS decreases rapidly being accompanied by swift muscle loss, both tapering off in the second and third week of disuse (Wall et al., 2013a,b). Therefore, assessing muscle protein synthesis at a later time point may miss important changes. In respect to nerve damage, the literature suggests a fairly steady rate of muscle loss (Goldspink, 1976; al-Amod

et al., 1991; Ma et al., 2007). It is important to note that the muscle continues to lose mass up to 3–12 months after nerve damage (Wu et al., 2014). To avoid any artifacts due to an initial inflammatory response induced by the surgery, we chose to analyze MPS during the second half of our intervention. We used D_2O as a tracer to measure integrated protein synthesis over the course of 2 weeks (Figure 3C). As opposed to a short term experiment with the constant infusion- or flooding method, this allowed us to assess chronic alterations of MPS.



To investigate changes in protein expression that may be underlying the observed changes in protein turnover, we analyzed key signaling proteins for muscle protein synthesis and breakdown. For muscle protein synthesis we focused on p70s6k1, a protein downstream of mTORC1, known to increase

protein synthesis upon phosphorylation and with a regulatory role in muscle growth (Baar and Esser, 1999; Saxton and Sabatini, 2017). To gain insight into the signaling underlying protein breakdown, we analyzed the E3 ubiquitin ligases MAFbx and MuRF1. These are muscle specific proteins downstream of FOXO, which have been shown to be upregulated under most atrophic conditions and are crucial regulators of muscle loss (Bodine et al., 2001; Gomes et al., 2001; Bodine and Baehr, 2014). In our model, protein expression of p70s6k1 is significantly increased in the nerve damaged leg compared to the control leg (Figure 5A, lower panel). The expression of p70s6k1 correlates with fractional synthesis rates of myofibrillar protein (Figure 6A). Interestingly that is still the case when expression and synthesis rates are analyzed exclusively in the control leg (Supplementary Figure 8). We tried to analyze phosphorylated p70s6k1, but failed to detect any in both, the damaged and the control legs. We confirmed the absence of phosphorylated p70s6k1 in our samples by the addition of positive controls (Supplementary Figure 6). The lack of phosphorylated p70s6k1 is not surprising, as the expression pattern appears to be transient and sampling of muscle would have to occur closely to the initiation of an early stimulus, which was not the case in our study (Ogasawara et al., 2013; West et al., 2016). Eventually, in case of our atrophy model the protein expression data seems to line up with the protein turnover data from the tracer experiments.



CONCLUSION

In summary, we found that nerve damage induced muscle loss is primarily based on muscle fiber atrophy, not the loss of muscle fibers. With the combination of integrating the D₂O tracer method with the analysis of absolute changes in muscle mass, we were able to find that in our model of muscle atrophy, muscle loss is accompanied by an increase as opposed to a decrease in MPS rates. These findings support the notion that muscle protein synthesis may be reflective of muscle remodeling and should not be used as a proxy to predict changes in muscle mass.

In conclusion, muscle atrophy caused by chronic constriction injury to the nerve is not associated with a decline in MPS rates.

AUTHOR CONTRIBUTIONS

HL was responsible for the design of the study, animal experiments, analysis of the samples, interpretation of the data, and writing of the manuscript. JS, HL, and AG prepared the samples for GC-MS analysis. LvL was involved in the design of the study, interpretation of the data, and writing of the manuscript. SK was involved in the interpretation of the data. SS was involved in the design of the study, interpretation of the data, and writing of the manuscript.

FUNDING

The study was supported by the German Research Foundation (DFG) through the International Research Training Group for Muscle Sciences (“MyoGrad” IGK1631) and a grant to SS and HL. The French-German University (UFA) supported HL through financial and educational support. Contributions were made possible by DFG funding through the Berlin-Brandenburg School for Regenerative Therapies (BSRT) GSC 203. The body composition analysis was performed at the

Phenotyping-Facility of the Max Delbrück Center for Molecular Medicine.

ACKNOWLEDGMENTS

We thank Adrienne Rothe, Monique Bergemann, Shoaib Afzal, and Christin Zasada for technical assistance. We would like to thank Andy Holwerda for helpful discussion of the project

REFERENCES

- al-Amood, W. S., Lewis, D. M., and Schmalbruch, H. (1991). Effects of chronic electrical stimulation on contractile properties of long-term denervated rat skeletal muscle. *J. Physiol.* 441, 243–256. doi: 10.1113/jphysiol.1991.sp018749
- Al-Majid, S., and McCarthy, D. O. (2001). Cancer-induced fatigue and skeletal muscle wasting: the role of exercise. *Biol. Res. Nurs.* 2, 186–197. doi: 10.1177/109980040100200304
- Baar, K., and Esser, K. (1999). Phosphorylation of p70S6 correlates with increased skeletal muscle mass following resistance exercise. *Am. J. Physiol. Cell Physiol.* 276, C120–C127. doi: 10.1152/ajpcell.1999.276.1.C120
- Baptista, A. F., Gomes, J. R., Oliveira, J. T., Santos, S. M., Vannier-Santos, M. A., and Martinez, A. (2008). High- and low-frequency transcutaneous electrical nerve stimulation delay sciatic nerve regeneration after crush lesion in the mouse. *J. Peripher. Nerv. Syst.* 13, 71–80. doi: 10.1111/j.1529-8027.2008.00160.x
- Bennett, G. J., and Xie, Y.-K. (1988). A peripheral mononeuropathy in rat that produces disorders of pain sensation like those seen in man. *Pain* 33, 87–107. doi: 10.1016/0304-3959(88)90209-6
- Bodine, S. C., and Baehr, L. M. (2014). Skeletal muscle atrophy and the E3 ubiquitin ligases MuRF1 and MAFbx/atrogin-1. *Am. J. Physiol. Endocrinol. Metab.* 307, E469–E484. doi: 10.1152/ajpendo.00204.2014
- Bodine, S. C., Latres, E., Baumhueter, S., Lai, V. K., Nunez, L., Clarke, B. A., et al. (2001). Identification of ubiquitin ligases required for skeletal muscle atrophy. *Science* 294, 1704–1708. doi: 10.1126/science.1065874
- Burd, N. A., Andrews, R. J., West, D. W., Little, J. P., Cochran, A. J., Hector, A. J., et al. (2012). Muscle time under tension during resistance exercise stimulates differential muscle protein sub-fractional synthetic responses in men. *J. Physiol.* 590, 351–362. doi: 10.1113/jphysiol.2011.221200
- Busch, R., Kim, Y. K., Neese, R. A., Schade-Serin, V., Collins, M., Awada, M., et al. (2006). Measurement of protein turnover rates by heavy water labeling of nonessential amino acids. *Biochim. Biophys. Acta* 1760, 730–744. doi: 10.1016/j.bbagen.2005.12.023
- Buse, M. G., McMaster, J., and Buse, J. (1965). The effect of denervation and insulin on protein synthesis in the isolated rat diaphragm. *Metab. Clin. Exp.* 14, 1220–1232. doi: 10.1016/0026-0495(65)90092-2
- Damas, F., Phillips, S. M., Libardi, C. A., Vechin, F. C., Lixandrão, M. E., Jannig, P. R., et al. (2016). Resistance training-induced changes in integrated myofibrillar protein synthesis are related to hypertrophy only after attenuation of muscle damage. *J. Physiol.* 594, 5209–5222. doi: 10.1113/JP272472
- Dyck, P. (2005). *Peripheral Neuropathy*. New York, NY: Elsevier Inc.
- Emery, P., Edwards, R., Rennie, M., Souhami, R., and Halliday, D. (1984). Protein synthesis in muscle measured in vivo in cachectic patients with cancer. *Br. Med. J.* 289, 584–586. doi: 10.1136/bmj.289.6445.584
- Engel, W. K., and Cunningham, G. G. (1963). Rapid examination of muscle tissue: An improved trichrome method for fresh-frozen biopsy sections. *Neurology* 13, 919–923. doi: 10.1212/WNL.13.11.919
- Frontera, W. R., and Ochala, J. (2015). Skeletal muscle: a brief review of structure and function. *Calcif. Tissue Int.* 96, 183–195. doi: 10.1007/s00223-014-9915-y
- Garber, K. (2016). *No Longer Going to Waste*. London: Nature Publishing Group.
- Gasier, H. G., Riechman, S. E., Wiggs, M. P., Previs, S. F., and Fluckey, J. D. (2009). A comparison of 2H₂O and phenylalanine flooding dose to investigate muscle protein synthesis with acute exercise in rats. *Am. J. Physiol. Endocrinol. Metab.* 297, E252–E259. doi: 10.1152/ajpendo.90872.2008
- Gigo-Benato, D., Russo, T. L., Geuna, S., Domingues, N. R., Salvini, T. F., and Parizotto, N. A. (2010). Electrical stimulation impairs early functional recovery

and design of the labeling protocol. We also thank Annette Schürmann for providing us with the GLUT4 antibody.

SUPPLEMENTARY MATERIAL

The Supplementary Material for this article can be found online at: <https://www.frontiersin.org/articles/10.3389/fphys.2018.01220/full#supplementary-material>

- and accentuates skeletal muscle atrophy after sciatic nerve crush injury in rats. *Muscle Nerve* 41, 685–693. doi: 10.1002/mus.21549
- Goldspink, D. (1976). The effects of denervation on protein turnover of rat skeletal muscle. *Biochem. J.* 156, 71–80. doi: 10.1042/bj1560071
- Goldspink, D. F. (1978). *Changes in the Size and Protein Turnover of the Soleus Muscle in Response to Immobilization or Denervation*. London: Portland Press Limited.
- Goldspink, D. F., Garlick, P. J., and McNurlan, M. (1983). Protein turnover measured in vivo and in vitro in muscles undergoing compensatory growth and subsequent denervation atrophy. *Biochem. J.* 210, 89–98. doi: 10.1042/bj2100089
- Gomes, M. D., Lecker, S. H., Jagoe, R. T., Navon, A., and Goldberg, A. L. (2001). Atrogin-1, a muscle-specific F-box protein highly expressed during muscle atrophy. *Proc. Nat. Acad. Sci.* 98, 14440–14445. doi: 10.1073/pnas.251541198
- Gregory, C. M., Vandenborne, K., and Dudley, G. A. (2001). Metabolic enzymes and phenotypic expression among human locomotor muscles. *Muscle Nerve* 24, 387–393. doi: 10.1002/1097-4598(200103)24:3<387::AID-MUS1010>3.0.CO;2-M
- Hector, A. J., McGlory, C., Damas, F., Mazara, N., Baker, S. K., and Phillips, S. M. (2018). Pronounced energy restriction with elevated protein intake results in no change in proteolysis and reductions in skeletal muscle protein synthesis that are mitigated by resistance exercise. *FASEB J.* 32, 265–275. doi: 10.1096/fj.201700158RR
- Lang, C. H., Frost, R. A., and Vary, T. C. (2007). Regulation of muscle protein synthesis during sepsis and inflammation. *Am. J. Physiol. Endocrinol. Metab.* 293, E453–E459. doi: 10.1152/ajpendo.00204.2007
- Ma, J., Shen, J., Garrett, J. P., Lee, C. A., Li, Z., Elsaïdi, G. A., et al. (2007). Gene expression of myogenic regulatory factors, nicotinic acetylcholine receptor subunits, and GAP-43 in skeletal muscle following denervation in a rat model. *J. Orthop. Res.* 25, 1498–1505. doi: 10.1002/jor.20414
- Marquis, K., Debigaré, R., Lacasse, Y., LeBlanc, P., Jobin, J., Carrier, G., et al. (2002). Midbody muscle cross-sectional area is a better predictor of mortality than body mass index in patients with chronic obstructive pulmonary disease. *Am. J. Respir. Crit. Care Med.* 166, 809–813. doi: 10.1164/rccm.2107031
- McKinnell, I. W., and Rudnicki, M. A. (2004). Molecular mechanisms of muscle atrophy. *Cell* 119, 907–910. doi: 10.1016/j.cell.2004.12.007
- Metter, E. J., Talbot, L. A., Schragger, M., and Conwit, R. (2002). Skeletal muscle strength as a predictor of all-cause mortality in healthy men. *J. Gerontol. A Biol. Sci. Med. Sci.* 57, B359–B365. doi: 10.1093/gerona/57.10.B359
- Mitchell, C. J., Churchward-Venne, T. A., Parise, G., Bellamy, L., Baker, S. K., Smith, K., et al. (2014). Acute post-exercise myofibrillar protein synthesis is not correlated with resistance training-induced muscle hypertrophy in young men. *PLoS One* 9:e89431. doi: 10.1371/journal.pone.0089431
- Ochala, J., Gustafson, A. M., Diez, M. L., Renaud, G., Li, M., Aare, S., et al. (2011). Preferential skeletal muscle myosin loss in response to mechanical silencing in a novel rat intensive care unit model: underlying mechanisms. *J. Physiol.* 589, 2007–2026. doi: 10.1113/jphysiol.2010.202044
- Ogasawara, R., Kobayashi, K., Tsutaki, A., Lee, K., Abe, T., Fujita, S., et al. (2013). mTOR signaling response to resistance exercise is altered by chronic resistance training and detraining in skeletal muscle. *J. Appl. Physiol.* 114, 934–940. doi: 10.1152/jappphysiol.01161.2012
- Ogilvie, R., and Feeback, D. (1990). Metachromatic dye ATPase method for the simultaneous identification of skeletal muscle fibers types I, II A, II B and II C. *Stain Technol.* 65, 231–241. doi: 10.3109/10520299009105613
- Phillips, S. M., and McGlory, C. (2014). Crosstalk proposal: the dominant mechanism causing disuse muscle atrophy is decreased protein

- synthesis. *J. Physiol.* 592, 5341–5343. doi: 10.1113/jphysiol.2014.273615
- Reid, M. B., Judge, A. R., and Bodine, S. C. (2014). Crosstalk opposing view: the dominant mechanism causing disuse muscle atrophy is proteolysis. *J. Physiol.* 592, 5345–5347. doi: 10.1113/jphysiol.2014.279406
- Rosenberg, I. H. (1997). Sarcopenia: origins and clinical relevance. *J. Nutr.* 127, 990S–991S. doi: 10.1093/jn/127.5.990S
- Sakurai, Y., Aarsland, A., Herndon, D. N., Chinkes, D. L., Pierre, E., Nguyen, T. T., et al. (1995). Stimulation of muscle protein synthesis by long-term insulin infusion in severely burned patients. *Ann. Surg.* 222, 283–294. doi: 10.1097/0000658-199509000-00007
- Saxton, R. A., and Sabatini, D. M. (2017). mTOR signaling in growth, metabolism, and disease. *Cell* 168, 960–976. doi: 10.1016/j.cell.2017.02.004
- Sepulveda, P. V., Bush, E. D., and Baar, K. (2015). Pharmacology of manipulating lean body mass. *Clin. Exp. Pharmacol. Physiol.* 42, 1–13. doi: 10.1111/1440-1681.12320
- Sommer, C. (2013). “Neuropathic pain model, chronic constriction injury,” in *Encyclopedia of Pain*, eds G. F. Gebhart and R. F. Schmidt (Heidelberg: Springer). doi: 10.1007/2F978-3-642-28753-4_2678
- Thomas, D. R. (2007). Loss of skeletal muscle mass in aging: examining the relationship of starvation, sarcopenia and cachexia. *Clin. Nutr.* 26, 389–399. doi: 10.1016/j.clnu.2007.03.008
- Trommelen, J., Holwerda, A. M., Kouw, I. W., Langer, H., Halson, S. L., Rollo, I., et al. (2016). Resistance exercise augments postprandial overnight muscle protein synthesis rates. *Med. Sci. Sports Exerc.* 48, 2517–2525. doi: 10.1249/MSS.0000000000001045
- Wall, B. T., Dirks, M. L., Snijders, T., van, Dijk JW, Fritsch, M., Verdijk, L. B., et al. (2016). Short-term muscle disuse lowers myofibrillar protein synthesis rates and induces anabolic resistance to protein ingestion. *Am. J. Physiol. Endocrinol. Metab.* 310, E137–E147. doi: 10.1152/ajpendo.00227.2015
- Wall, B. T., Dirks, M. L., and van Loon, L. J. (2013a). Skeletal muscle atrophy during short-term disuse: implications for age-related sarcopenia. *Ageing Res. Rev.* 12, 898–906. doi: 10.1016/j.arr.2013.07.003
- Wall, B. T., Snijders, T., Senden, J. M., Ottenbros, C. L., Gijsen, A. P., Verdijk, L. B., et al. (2013b). Disuse impairs the muscle protein synthetic response to protein ingestion in healthy men. *J. Clin. Endocrinol. Metab.* 98, 4872–4881. doi: 10.1210/jc.2013-2098
- Wannamethee, S. G., Shaper, A. G., Lennon, L., and Whincup, P. H. (2007). Decreased muscle mass and increased central adiposity are independently related to mortality in older men. *Am. J. Clin. Nutr.* 86, 1339–1346. doi: 10.1093/ajcn/86.5.1339
- West, D. W., Baehr, L. M., Marcotte, G. R., Chason, C. M., Tolento, L., Gomes, A. V., et al. (2016). Acute resistance exercise activates rapamycin-sensitive and-insensitive mechanisms that control translational activity and capacity in skeletal muscle. *J. Physiol.* 594, 453–468. doi: 10.1113/JP271365
- Wilkinson, D. J., Franconi, M. V., Brook, M. S., Narici, M. V., Williams, J. P., Mitchell, W. K., et al. (2014). A validation of the application of D(2)O stable isotope tracer techniques for monitoring day-to-day changes in muscle protein subfraction synthesis in humans. *Am. J. Physiol. Endocrinol. Metab.* 306, E571–E579. doi: 10.1152/ajpendo.00650.2013
- Wu, P., Chawla, A., Spinner, R. J., Yu, C., Yaszemski, M. J., Windebank, A. J., et al. (2014). Key changes in denervated muscles and their impact on regeneration and reinnervation. *Neural Regen. Res.* 9, 1796–1809. doi: 10.4103/1673-5374.143424
- Yarasheski, K. E., Zachwieja, J. J., and Bier, D. M. (1993). Acute effects of resistance exercise on muscle protein synthesis rate in young and elderly men and women. *Am. J. Physiol.* 265, E210–E214. doi: 10.1152/ajpendo.1993.265.2.E210

Conflict of Interest Statement: The authors declare that the research was conducted in the absence of any commercial or financial relationships that could be construed as a potential conflict of interest.

Copyright © 2018 Langer, Senden, Gijsen, Kempa, van Loon and Spuler. This is an open-access article distributed under the terms of the Creative Commons Attribution License (CC BY). The use, distribution or reproduction in other forums is permitted, provided the original author(s) and the copyright owner(s) are credited and that the original publication in this journal is cited, in accordance with accepted academic practice. No use, distribution or reproduction is permitted which does not comply with these terms.

CURRICULUM VITAE

"Mein Lebenslauf wird aus datenschutzrechtlichen Gründen in der elektronischen Version meiner Arbeit nicht veröffentlicht."

LIST OF PUBLICATIONS

1. Langer HT, Mossakowski AA, Willis BJ, Grimsrud KN, Wood JA, Lloyd KCK, Zbinden-Foncea H, Baar K. Generation of Desminopathy in Rats using CRISPR-Cas9. *J Cachexia Sarcopenia Muscle*. 2020 Oct;11(5):1364-1376. doi: 10.1002/jcsm.12619. Epub 2020 Sep 7.
2. Jannas-Vela S, Langer HT, Marambio H, Baar K, Zbinden-Foncea H. Effect of a 12-week endurance training program on force transfer and membrane integrity proteins in lean, obese, and type 2 diabetic subjects. *Physiol Rep*. 2020 May;8(9):e14429. doi: 10.14814/phy2.14429.
3. Langer HT, Afzal S, Kempa S, Spuler S. Nerve damage induced skeletal muscle atrophy is associated with increased accumulation of intramuscular glucose and polyol pathway intermediates. *Sci Rep*. 2020 Feb 5;10(1):1908. doi: 10.1038/s41598-020-58213-1.
4. Langer HT, Mossakowski AA, Baar K, et al. Commentaries on Viewpoint: Rejuvenation of the term sarcopenia. *J Appl Physiol (1985)*. 2019 Jan 1;126(1):257-262. doi: 10.1152/japophysiol.00816.2018.
5. Langer HT, Senden JMG, Gijsen AP, Kempa S, van Loon LJC, Spuler S. Muscle Atrophy Due to Nerve Damage Is Accompanied by Elevated Myofibrillar Protein Synthesis Rates. *Front Physiol*. 2018 Aug 31;9:1220. doi: 10.3389/fphys.2018.01220.
6. Langer HT. Master and commander? FoxO's role in muscle atrophy. *J Physiol*. 2017 May 10. doi: 10.1113/JP274554.
7. Trommelen J, Holwerda AM, Kouw IW, Langer H, Halson SL, Rollo I, Verdijk LB, van Loon LJ. Resistance Exercise Augments Postprandial Overnight Muscle Protein Synthesis Rates. *Med Sci Sports Exerc*. 2016 Dec;48(12):2517-2525.
8. Gorissen SHM, Horstman AMH, Franssen R, Crombag JJR, Langer H, Bierau J, Respondek F, van Loon LJC. Ingestion of Wheat Protein Increases In Vivo Muscle Protein Synthesis Rates in Healthy Older Men in a Randomized Trial. *J Nutr*. 2016 Sep;146(9):1651-9.
9. Gorissen SH, Respondek F, Franssen R, Crombag JJ, Langer H, Horstman AM, van Loon LJ. MON-PP030: The Anabolic Properties of Wheat Protein Hydrolysate Compared to Casein and Whey. *Clinical Nutrition Volume 34, Supplement 1, September 2015, Pages S138–S139*.
10. Langer H, Carlsohn A. The effect of different dietary proteins on skeletal muscle hypertrophy in young men: a systematic review. *J Strength Cond Res*. June 2014 - Volume 36 - Issue 3 - p 33-42.
11. Ahmed MS, Langer H, Abed M, Voelkl J, Lang F. The uremic toxin acrolein promotes suicidal erythrocyte death. *Kidney Blood Press Res*. 2013;37(2-3):158-67.

ACKNOWLEDGEMENTS

On my journey to obtain a PhD in biology I have encountered many remarkable and amazing people who have shaped my path. In no way comprehensive, in the following I would like to take the chance to single out a few particularly influential people and thank them.

Zuerst möchte ich meinen Eltern Helga und Helge danken. Ohne eure Hilfe und Unterstützung wäre nichts von all dem möglich gewesen. Viel wichtiger noch als der akademische Erfolg, möchte ich euch dafür zu danken mich zu dem Menschen gemacht zu haben, der ich bin. Mit einer Mischung aus Forderung und Förderung hatte ich zu jedem Zeitpunkt das Gefühl geliebt zu sein und den Raum zu haben mich selbst zu verwirklichen. Danke für eure Geduld und euren Glauben. Gleiches gilt für Helen – danke für die schwesterliche Unterstützung. Außerdem möchte ich meinen Großmüttern und insbesondere Ingeborg für Ihren Rückhalt danken.

Als nächstes möchte ich meiner akademischen Familie und allen voran meiner Doktormutter Simone danken. Simone, vielen Dank für dein großes Vertrauen und die bedingungslose Unterstützung. Dein Wille jungen Forschern die Chance zu bieten Fuß in der Wissenschaft zu fassen und dein Engagement für MyoGrad sind unglaublich bewundernswert. Insbesondere im Angesicht von administrativen oder finanziellen Risiken, wie in meinem Falle. Ich weiß, dass ich vor allem dir die Chance verdanke in Buch den nächsten Schritt auf der akademischen Leiter gemacht zu haben und bin dir dafür ewig dankbar. Danke für deine Ratschläge und die Führung.

Außerdem möchte ich gerne den restlichen AG Spuler Mitgliedern danken. Allen voran Eric, mit dem ich Tag für Tag und Woche für Woche anregende Gespräche in der Mensa hatte und so gut wie jedes Mal im Anschlag das Internet konsultieren musste um meinen Horizont zu erweitern. Ich bin sehr glücklich im Laufe der Zeit das Mittagessen zu einem Feierabend Bier erweitert zu haben. Außerdem gilt mein Dank Verena und Tobi, die mir insbesondere zu Beginn meiner Promotion mit Rat und Tat zur Seite standen. Weiterhin möchte ich gerne Monique und Adrienne für Ihre Hilfe während der Tierexperimente danken. Außerdem gilt mein Dank auch Andreas, der immer bereit war mich in meinen Überlegungen mit wertvollem Rat zu unterstützen. Zu guter Letzt möchte ich mich ganz besonders bei Susanne bedanken. Unbeirrbar und grenzenlos hilfsbereit bin ich nicht der erste Doktorand, der ohne deine Hilfe verloren gewesen wäre. Danke dafür.

Nach Simone und der AG Spuler möchte ich gerne meinem Doktorvater Stefan danken. Du hast dich unmittelbar auf Simones Wort und Vertrauen in mich verlassen und mir wie selbstverständlich die Möglichkeit gegeben in deinem Labor einen Großteil der Daten dieser Dissertation zu generieren. Ich durfte von dir und in deinem Labor unglaublich viel lernen und möchte dir für den Raum zur Selbstverwirklichung und deine Ratschläge danken. Im Zusammenhang mit der AG Kempa gilt mein Dank außerdem Christin, Fardad, Nadine, Matthias und Henning, die mich während meiner ersten Schritte in der MAUI Welt und am GC-MS an der Hand genommen und stets geduldig meine Anfänger-Fragen beantwortet haben. Insbesondere die AG Kempa Retreats und Weihnachtsfeiern werden immer einen Platz in meinem Herzen haben.

Vielen Dank auch an die Werkstatt des MDC und deren Mitarbeiter. Vom Platindraht zum Umgang mit dem LaGeTSi, ohne Sie wären meine elektrophysiologischen Versuche unmöglich gewesen.

Over the years prior to and during my PhD, I was lucky enough to have been supported and mentored by great scientists all over the world. This includes Professor Keith Baar at the University of California, who ended up having to deal with me again now that I took on a postdoc position in his lab. Thank you, Keith, for paving the way for me to become a scientist. Your guidance, such as the advice to visit

Florian Lang in Tübingen and doing my Master with Luc, has always been of incredible value. What's even more important, your passion for muscle science was what inspired me to become a scientist in the first place. Thank you for that. I would also like to thank Professor Shaffrath for his teaching efforts and the openness towards a keen, but potentially annoying exchange student from Germany.

Of course, I also have to thank Luc van Loon. Dear Luc, thank you for working with me even though I invaded your office. Your advice and guidance were invaluable during my MSc and even more so during my PhD. While I haven't been your PhD student officially, in many ways you were still a real supervisor to me – for which I will be forever grateful. And since we are talking about M3 now, I would also like to thank Andy for the helpful discussions of my project and the D2O labeling. I am also grateful and indebted to Joan, Annemie and Joy for their technical assistance. You guys are a great lab!

Abseits der professionellen Unterstützung möchte ich gerne meinen Freunden für Ihren Rückhalt danken. Die Liste hier ist lang, wofür ich mich besonders glücklich schätze. Sei es die alte Waldschul-Clique um Pia, Becci und Baris, Zwolly oder Mani, der schon seit Grundschulzeiten an meiner Seite ist. Mein Dank gilt außerdem Constanze, die mich in meinem akademischen Streben immer bedingungslos unterstützt und während eines wesentlichen Teiles meiner Promotion begleitet hat. Weiterhin will ich gerne Harry, Sophie und vor allem Jann dafür danken, dass ihr mir abseits des Labores geholfen habt nicht den Verstand zu verlieren.

Besonders großer Dank gilt außerdem natürlich Fabi. Als bester Freund bist du seit Kindergartenzeiten der allerwichtigste Rückhalt. Vielen Dank für die vielen Stunden Fastfood-befuehrter Gespräche, in denen wir über alle relevanten und irrelevanten Dinge des Lebens philosophiert haben. Ich denke es ist fair zu sagen, dass du mich stärker beeinflusst hast als jeder andere Mensch und ich ohne dich nicht der wäre, der ich bin.

Abschließend möchte ich mich gerne bei Agata bedanken. Ich hatte das unsagbare Glück Dich im Zusammenhang mit meiner Promotion kennenlernen zu dürfen. Du hast mein Leben jedoch weit stärker verändert als die Aussicht zweier Buchstaben vor meinem Namen. Mein Blitzschlag. Danke für deine genialen Ideen, die so gut wie immer begründete Skepsis und deine immer hilfreichen Ratschläge. Insbesondere in der finalen Phase dieser Dissertation. Du inspirierst mich!